PNAS
www.pnas.org

Supplementary Information for

Repurposing type III polyketide synthase a malonyl-CoA biosensor for metabolic engineering in bacteria

Dongsoo Yang, Won Jun Kim, Seung Min Yoo, Jong Hyun Choi, Shin Hee Ha, Mun Hee Lee and Sang Yup Lee

Correspondence should be addressed to: Sang Yup Lee
Email: leesy@kaist.ac.kr

This PDF file includes:

Materials and Methods
Texts S1 to S8
Figs. S1 to S16
Tables S1 to S5
References for SI reference citations

Other supplementary materials for this manuscript include the following:

Dataset S1 to S2

www.pnas.org/cgi/doi/10.1073/pnas.1808567115

SI Appendix Materials and Methods

Materials. Cerulenin and resveratrol were purchased from Sigma-Aldrich. 6-Methylsalicylic acid was from Acros Organics, naringenin was from Tokyo Chemical Industry. Genes encoding AaPCSm, AaOKS, AaPKS4, AaPKS5, RpALS, AaPKS3, VvSTS and PhCHS were synthesized as gBlocks Gene Fragments from Integrated DNA Technologies Inc. (Skokie, IL). The commercial aloe powder was purchased from Ecofactory (Pyeongtaek, Republic of Korea).

Plasmid construction. Standard protocols were used for PCR, gel electrophoresis and transformation experiments (1). The plasmids and oligonucleotides used in this study are listed in Table S4 and S5, respectively. *E. coli* DH5α (Invitrogen) was used as a host strain for routine gene cloning, in Luria-Bertani (LB) medium (per liter: 10 g tryptone, 5 g yeast extract and 10 g NaCl) or on LB agar plates (1.5% agar, w/v) at 37°C supplemented with appropriate concentrations of antibiotics when necessary: 50 μg/mL of kanamycin, 100 μg/mL of ampicillin and/or 100 μg/mL of spectinomycin. Polymerases used for PCR reactions were either Lamp-Pfu or Pfu purchased from Biofact (Daejeon, Republic of Korea). Restriction endonucleases and T4 polynucleotide kinase (PNK) were purchased from either Enzynomics (Daejeon, Republic of Korea) or NEB (Ipswich, MA). For the construction of the plasmid pET-Sgr_rppA, the *rppA* gene was PCR amplified from the genomic DNA of *Streptomyces griseus* subsp. *griseus* using the primers Sgr_rppA_F and Sgr_rppA_R. Then the amplified *rppA* gene was inserted into pET-30a(+) at EcoRI and BamHI sites using Gibson assembly (2). Construction of the plasmids harboring various *rppA* genes from different sources (pET-Sco_rppA, pET-Sma_rppA, pET-Sen_rppA, pET-Sp_rppA, pET-Sac_rppA) was conducted in the same way. The corresponding primer pairs listed in Table S5 were used. For testing coexpression of WhiE_ORFII on flaviolin production, plasmid pET-Sgr_rppA-whiE was constructed. The gene fragment was amplified from the genomic DNA of *Streptomyces*

coelicolor using the primers whiE_orfII_F (containing ribosome binding site) and whiE_orfII_R, and was inserted into the vector pET-Sgr_rppA at EcoRI and HindIII sites. To construct pTacCDFS, the platform plasmid harboring CDF origin, spectinomycin-resistance marker and multiple cloning site (MCS) under *tac* promoter was amplified from pTac15K plasmid (3) using the primers pTac_CDF_F and pTac_CDF_R. This DNA fragment was then assembled with the linearized pCDFDuet-1 (Novagen) plasmid backbone (amplified using the primers pCDF_pTac_IV_F and pCDF_pTac_IV_R) using Gibson assembly. The platform plasmid pTrcCDFS harboring CDF origin, spectinomycin resistance marker and MCS under *trc* promoter was constructed in the same way except that pTrc99A plasmid (3) was utilized as the template for amplifying the insertion DNA fragment. To change the *rppA* expression vector, the plasmid pTac-Sgr_rppA was constructed by inserting the *rppA* gene into the plasmid pTacCDFS. The *rppA* gene was amplified from the genomic DNA of *S. griseus* with the primers pTac_rppA_F and pTac_rppA_R, and inverse PCR was conducted with the plasmid pTacCDFS using the primers pTac_rppA_IV_F and pTac_rppA_IV_R. These two DNA fragments were Gibson assembled to form the plasmid pTac-Sgr_rppA. For improved expression of *rppA*, optimized 5' untranslated region (5'UTR) sequence was obtained by using the UTR designer developed by Seo et al. (url: https://sbi.postech.ac.kr/utr_designer/) (4). For the input protein coding sequence, the first 36 bp DNA sequence of the *S. griseus rppA* gene was used. Among the output 5'UTRs, the sequence with the highest predicted expression level was utilized. The vector pTac-5'UTR-Sgr_rppA was constructed by inverse PCR amplification of the vector pTac-Sgr_rppA using the primers pTac_rppA_IV_F and pTac_rppA_UTR_IV_R followed by digestion with DpnI restriction endonuclease and consequent ligation of the linearized vector with T4 PNK and T4 ligase.

To test other type III polyketide synthases whether they could also be used as malonyl-CoA biosensors, plasmids pET-AaPCSm, pET-AaOKS, pET-AaPKS3m, pET-AaPKS4 and

pET-AaPKS5 were constructed using the same method used for the construction of pET-30a(+)-based plasmids harboring *rppA* genes described above. For the construction of the plasmid pET-AaPCSm, the *AaPCSm* gene was PCR amplified from the artificially synthesized *AaPCSm* DNA fragment using the primers AaPCS_F and AaPCS_R. Then the amplified *AaPCSm* gene was inserted into pET-30a(+) at NdeI and EcoRI sites using Gibson assembly (2). Construction of the other plasmids was conducted in the same way. The corresponding primer pairs listed in Table S5 were used. In the case of pET-AaPKS3m, however, since the *AaPKS3* gene was artificially synthesized, plasmid pET-AaPKS3 harboring native *AaPKS3* gene was firstly constructed. Then, site-directed mutagenesis was conducted for this plasmid using the primers AaPKS3_mut_F and AaPKS3_mut_R to construct the plasmid pET-AaPKS3m harboring the mutant *AaPKS3m* gene.

To construct the vectors for *rppA* expression in *Pseudomonas putida*, pBBR1MCS2 was used as the base plasmid. This plasmid was linearized by inverse PCR using the primers pTac_pBBR1_IV_F and pTac_pBBR1_IV_R. P*tac*-based *rppA* expression cassette was amplified from the plasmid pTac-Sgr_rppA using the primers pTac_pBBR1_F and pTac_pBBR1_R. This amplified gene fragment was assembled with the linearized pBBR1MCS2 plasmid by Gibson assembly to yield the plasmid pBBR1-rppA. In order to test whether N-terminal poly-histidine(His)-tag aids in RppA expression (5), the vector pTac-His-Sgr_rppA was constructed. The gene coding N-terminal His-tagged RppA was amplified from the genomic DNA of *S. griseus* using the primers pTac_His_rppA_F and pTac_rppA_R. This gene fragment was assembled, by Gibson assembly, with the plasmid pTacCDFS linearized by inverse PCR using the primers pTac_rppA_IV_F and pTac_rppA_IV_R. Then, the resultant plasmid pTac-His-Sgr_rppA was amplified using the primers pTac_pBBR1_F and pTac_pBBR1_R, and was assembled with the linearized pBBR1MCS2 plasmid by Gibson assembly to yield the plasmid pBBR1-His-rppA. To construct the vectors for *rppA* expression

in *Corynebacterium glutamicum*, pCES-H36 was used as the base plasmid. To linearize this plasmid, pCES-H36-GFP was amplified by inverse PCR using the primers pCES_H36_IV_F and pCES_H36_IV_R. P*tac*-based *rppA* expression cassette was amplified from the plasmid pTac-Sgr_rppA using the primers pCES_rppA_F and pCES_rppA_R. P*tac*-based N-terminal poly-His-tagged *rppA* expression cassette was amplified from the plasmid pTac-His-Sgr_rppA using the primers pCES_His_rppA_F and pCES_rppA_R. These two gene fragments were each assembled with the linearized pCES-H36 plasmid to yield the plasmids pCES-rppA and pCES-His-rppA, respectively.

To test the effects of overexpressing FVSEOF gene targets, individual genes were each cloned into the plasmid pTrc99A. Using the genomic DNA of *E. coli* W3110 as the template, PCR amplification was conducted by using the corresponding primer pairs listed in Table S5. Then, inverse PCR was conducted with pTrc99A as the template using the primers pTrc_IV_F and pTrc_IV_R. After DpnI treatment of the inverse PCR products, the two DNA fragments were assembled using Gibson assembly to yield the plasmids pTrc99A-zwf, pTrc99A-mdh, pTrc99A-fumA, pTrc99A-fumB, pTrc99A-fumC, pTrc99A-serA, pTrc99A-serB, pTrc99A-serC and pTrc99A-tpiA.

To construct pTac-Pg6MSAS, pTac15K was used as the template for inverse PCR using the primer pair pTac_6MSAS_IV_F and pTac_6MSAS_IV_R followed by DpnI treatment. Then, *Pg6MSAS* was amplified using the genomic DNA of *Penicillium griseofulvum* by consecutive PCR reactions using the primers 6MSAS_F_1 and 6MSAS_R, then using 6MSAS_F_2 and 6MSAS_R. This DNA fragment was inserted into the linearized pTac15K plasmid by Gibson assembly. Before inserting *Bacillus subtilis sfp* gene into the plasmid pTac-Pg6MSAS, pTac15K-sfp plasmid was constructed by inserting the *sfp* gene amplified from the genomic DNA of *B. subtilis* using the primers sfp_F and sfp_R into the pTac15K plasmid at EcoRI site. The plasmid pTac-Pg6MSAS-sfp was constructed by inserting the *sfp* gene

fragment amplified from pTac15K-sfp using the primers pTac_sfp_F and pTac_sfp_R into the plasmid pTac-Pg6MSAS at SphI site. For the production of aloesone, the direct aglycone precursor of aloesin, pCDF-RpALS and pCDF-AaPKS3 were constructed by inserting artificially synthesized *Rheum palmatum ALS* and *Aloe arborescens PKS3* DNA fragments into the pCDFDuet-1 plasmid at NcoI site by Gibson assembly.

Plasmid pBBR1TaC harboring *tac* promoter-based gene expression cassette was constructed from pBBR1MCS plasmid as follows. The plasmid pBBR1MCS was linearized by inverse PCR using the primers pBBR1TaC_IV_F and pBBR1TaC_IV_R, and was treated with DpnI restriction endonuclease. Then, using pTac15K plasmid as template, DNA fragment composed of *tac* promoter, MCS and *rrnBT1T2* terminator was amplified using the primers pBBR1TaC_F and pBBR1TaC_R. This amplified DNA fragment was assembled with the linearized pBBR1MCS plasmid by Gibson assembly, resulting in the plasmid pBBR1TaC. For increased production of 6MSA and aloesone, gene expression cassettes from the plasmids pTrc99A-zwf, pTrc99A-mdh and pTrc99A-serA were moved to pBBR1TaC. Each of the *zwf*, *mdh* and *serA* gene fragments was amplified from the respective plasmids by using the primers pTac_frag_F and pTac_frag_R. The plasmid pBBR1TaC was linearized by PCR using the primers pTaC_IV_F and pTaC_IV_R, treated with DpnI endonuclease, and was assembled with the *zwf*, *mdh* and *serA* gene fragments using Gibson assembly to yield the plasmids pBBR1-zwf, pBBR1-mdh and pBBR1-serA. To overexpress *C. glutamicum* acetyl-CoA carboxylase, the two large subunits alpha (encoded by *accBC*) and beta (encoded by *accD1*; previously *dtsR1*) were individually cloned into pBBR1TaC. First, pBBR1TaC was linearized by inverse PCR using the primers pTac_rppA_IV_F and pTac_rppA_IV_R and was treated with DpnI restriction endonuclease to eliminate the plasmid template. Then, *accBC* was amplified by PCR using the primers Cgl_accBC_F and Cgl_accBC_R, and *accD1* was amplified by PCR using the primers Cgl_accD1_F and Cgl_accD1_R. These two DNA

fragments were each assembled with the linearized pBBR1TaC by Gibson assembly to yield the plasmids pBBR1-accBC and pBBR1-accD1. To construct the plasmid pBBR1-accBCD1 harboring both *accBC* and *accD1*, *accD1* gene fragment was PCR amplified from the plasmid pBBR1-accD1 using the primers pTac_HindIII_frag_F and pTac_HindIII_frag_R and was Gibson assembled with the HindIII-digested plasmid pBBR1-accBC. To overexpress pyruvate dehydrogenase, the three subunits E1 (encoded by *aceE*), E2 (encoded by *aceF*) and E3 (encoded by *lpd*) were individually cloned into pBBR1TaC. First, *aceEF* was PCR amplified using the primers aceEF_F and aceEF_R, and *lpd* was PCR amplified using the primers lpd_F and lpd_R. These two DNA fragments were each assembled with the previously linearized pBBR1TaC by Gibson assembly to yield the plasmids pBBR1-aceEF and pBBR1-lpd. To construct the plasmid pBBR1-aceEF-lpd harboring both *aceEF* and *lpd*, *lpd* gene fragment was PCR amplified from the plasmid pBBR1-lpd using the primers pTac_SalI_frag_F and pTac_SalI_frag_R and was Gibson assembled with the SalI digested plasmid pBBR1-aceEF. To construct the plasmids pBBR1-gapA, pBBR1-pgk and pBBR1-acs, the *gapA*, *pgk* and *acs* gene fragments were each amplified from the genomic DNA of *E. coli* BL21 using the primer sets gapA_F and gapA_R, pgk_F and pgk_R, and acs_F and acs_R. Each of these gene fragments was assembled with the previously linearized pBBR1TaC to yield the corresponding plasmids.

For *p*-coumaric acid production, we constructed vector sets for the expression of SeTAL: pTrc-SeTAL, pTrc-HisTAL, pTrc-TrxTAL. For the construction of pTrc-SeTAL, 5'UTR optimization was conducted by applying the same method and conditions used for optimizing the 5'UTR of *Sgr_rppA*. PCR amplification of the *SeTAL* gene was conducted using the genomic DNA of *Saccharothrix espanaensis* as the template and using the primers SeTAL_F and SeTAL_R. Then pTrc99A was linearized by inverse PCR using the primers pTrc99A_IV_F and pTrc99A_IV_R, DpnI treated and assembled with the *SeTAL* fragment

using Gibson assembly to yield pTrc-SeTAL. As N-terminal poly-His-tag is reported to potentially aid in target enzyme expression (5), extending poly-His-tag after the start codon of the *SeTAL* gene was attempted. Thus, this gene fragment was amplified using the genomic DNA of *S. espanaensis* as the template and using the primers HisTAL_F and SeTAL_R. Then, the constructed pTrc-SeTAL was linearized by inverse PCR using the primers pTrc99A_IV_F and pTrcTAL_IV_R and was DpnI treated. These DNA fragments were Gibson assembled to yield the plasmid pTrc-HisTAL. For the construction of pTrc-TrxTAL, the *trxA* gene was amplified from the genomic DNA of *E. coli* W3110 using the primers TrxA_F and TrxA_R, along with the amplification of TAL using the primers TrxTAL_F and SeTAL_frag_R. Then, overlap extention PCR was conducted to produce the fused DNA fragment consists of *SeTAL* and *trxA* using the primers TrxA_ext_F and SeTAL_R. Then, this fused DNA fragment was assembled with the linearized pTrc99A (used for pTrc-HisTAL construction) using Gibson assembly, to yield the plasmid pTrc-TrxTAL. For the construction of the vector pTY13-HisTAL, we first amplified the HisTAL expression cassette which consists of P*trc*-rbs-*HisTAL-rrnBT1T2*$_T$, using the primers pTac_frag_NheI_F and pTac_frag_NheI_R. This DNA fragment was then inserted into the vector pTY13 at NheI site by Gibson assembly.

Then, for the conversion of *p*-coumaric acid to *p*-coumaroyl-CoA, the *At4CL1* gene was amplified from the cDNA of *Arabidopsis thaliana* using the primers At4CL1_F and At4CL1_R. The amplified gene was inserted into the pTac15K plasmid at EcoRI and KpnI sites using Gibson assembly, to yield pTac-At4CL1. Then, the plasmid harboring the mutated *At4CL1* (*At4CL1m*) was cloned by three consecutive rounds of site-directed mutagenesis. First site-directed mutagenesis was conducted by using the primers At4CL1_mut_F_1 and At4CL1_mut_R_1. For the second and third reactions, the primer sets At4CL1_mut_F_2 / At4CL1_mut_R_2 and At4CL1_mut_F_3 / At4CL1_mut_R_3 were used, with the plasmid pTac-At4CL1m as the resultant construct. In order to compare different *4CL* genes, additional

plasmids for the expression of *At4CL3, At4CL4* and *Sc4CLm* were constructed. From the cDNA of *A. thaliana, At4CL3* and *At4CL4* were amplified using the primers At4CL3_F / At4CL3_R and At4CL4_F / At4CL4_R, and each gene fragment was inserted into pTac15K at EcoRI and KpnI sites by Gibson assembly. Thus, the vectors pTac-At4CL3 and pTac-At4CL4 were constructed. From the genomic DNA of *S. coelicolor*, *Sc4CL* was amplified using the primers Sc4CL_F and Sc4CL_R and was inserted into pTac15K at EcoRI and KpnI sites by Gibson assembly. Then, site-directed mutagenesis was conducted using the primers Sc4CL_mut_F and Sc4CL_mut_R. Thus, the vector pTac-Sc4CLm was constructed. Construction of the plasmid pTac-VvSTS was conducted similarly. The artificially codon optimized and synthesized *VvSTS* fragment was amplified using the primers VvSTS_F and VvSTS_R and inserted at EcoRI and KpnI sites of pTac15K by Gibson assembly. Then, pTac15K-based vectors harboring different combinations of the *4CL* genes and the *VvSTS* gene were constructed. The *VvSTS* gene expression cassette, which consists of P*tac*-rbs-*VvSTS*-*rrnBT1T2*$_T$, was amplified using the primers pTac_frag_NheI_F and pTac_frag_NheI_R and was inserted at NheI site of the plasmids pTac-At4CL3, pTac-At4CL4 and pTac-Sc4CLm by Gibson assembly to yield the plasmids pTac-VvSTS-At4CL3, pTac-VvSTS-At4CL4 and pTac-VvSTS-Sc4CLm, respectively. For the case of *At4CL1m*, the *At4CL1m* expression cassette was amplified using the primers pTac_PvuII_frag_F and pTac_PvuII_frag_R and was inserted at PvuII site of the plasmid pTac-VvSTS by Gibson assembly to yield the plasmid pTac-VvSTS-At4CL1m. To test various genetic constructs for the expression of *VvSTS* and *At4CL1m*, expressing the two genes in an operon and fusing the two genes were attempted. Construction of the plasmid pTac-At4CL1m-opr-VvSTS was conducted by amplifying the *VvSTS* gene using the primers VvSTS_opr_F and VvSTS_opr_R, and inserting the DNA fragment into the pTac-At4CL1m plasmid at SphI site. Construction of the plasmid pTac-At4CL1m-fus-VvSTS was conducted by amplifying the *At4CL1m* gene using the primers At4CL1_fus_F and At4CL1_fus_R, and

inserting the DNA fragment into the pTac-VvSTS plasmid at NdeI site. For the peptide linker between At4CL1 and VvSTS, flexible glycine-serine linker (Gly-Gly-Gly-Ser) was used. Since the expression platform vector for resveratrol production has to be compatible with the pTY13-HisTAL plasmid to allow *p*-coumaric acid production from glucose/glycerol, the expression cassette of the best resveratrol producer (P*tac*-VvSTS-At4CL1m) was moved to pTacCDFS. The *VvSTS* expression cassette comprised of P*tac*-rbs-*VvSTS-rrnBT1T2*$_T$ was amplified using the primers pTac_frag_F and pTac_frag_R, and was Gibson assembled with the linearized pTacCDFS plasmid amplified with the primers pTaC_IV_F and pTaC_IV_R. The resultant vector was digested with PstI restriction endonuclease and was inserted with *At4CL1m* expression cassette amplified from the plasmid pTac-At4CL1m using the primers At4CL1m_PstI_F and At4CL1m-PstI_R, either by ligation or Gibson assembly, resulting in the plasmid pTacCDF-VvSTS-At4CL1m.

For the construction of plasmids harboring the naringenin biosynthetic pathway, *At4CL1m* was firstly amplified with the primers At4CL1_KpnI_F and At4CL1_OE_R. *AtCHI* was amplified using the primers AtCHI_OE_F and AtCHI_BamHI_R using the cDNA of *A. thaliana* as the template. Overlap extension PCR of the *At4CL1m* and *AtCHI* DNA fragments were conducted using the primers At4CL1_KpnI_F and AtCHI_BamHI_R, and the resultant DNA fragment was inserted into pTrc99A at KpnI and BamHI sites. Then, *PhCHS* was amplified using the primers PhCHS_BamHI_F and PhCHS_XbaI_R using the artificially synthesized *Petunia x hybrida CHS* as the template, and was inserted into the previously constructed vector at BamHI and XbaI sites to yield the vector pTrc-At4CL1m-AtCHI-PsCHS. However, since we could not utilize the pTrc99A-based vector system due to plasmid compatibility issue, we decided to move the whole gene cassettes to pTrcCDFS. Thus, we isolated the whole operon for naringenin biosynthesis by digesting the pTrc-At4CL1m-AtCHI-PsCHS vector with NcoI and PstI. The plasmid pTrcCDFS was linearized by inverse PCR

using the primers pTrc_NcoI_IV_R and pTrc_PstI_IV_F. The two DNA fragments were assembled using Gibson assembly to yield the vector pTrcCDF-At4CL1m-AtCHI-PhCHS.

All DNA sequences of the plasmid constructs listed in this study were confirmed by either Macrogen (Seoul, Republic of Korea) or Bionics (Daejeon, Republic of Korea). We uploaded the sequences of most of the plasmids used in this study to GenBank and added the corresponding accession numbers to the plasmid list in Table S4.

***E. coli* genome-scale synthetic sRNA library construction.** To construct the *E. coli* genome-scale synthetic sRNA library, the pWAS plasmid reported in our previous paper was utilized (6, 7). Target-binding sequences complementary to the first 24-bp of each target gene was inserted between the scaffold and the P_R promoter by site-directed mutagenesis; first, inverse PCR using pWAS as the template was conducted for each target gene. The forward primers were designed to bind to the 5'-end 22 bp of *micC* scaffold region with the reverse complementary DNA sequence of 1^{st}-12^{th} bases of each target gene (from the start codon) as extended arms. The reverse primers were designed to bind to the 3'-end 19 bp of P_R promoter region with the DNA sequence of 13^{th}-24^{th} bases of each target gene (from the start codon) as extended arms. Each amplified PCR product was then purified and digested with DpnI for template (pWAS) degradation. When using DpnI, template plasmid should not be prepared from methylase-deficient strains such as JM110 since DpnI digests methylated adenines in the GATC sequence. After DpnI treatment, the linearized DNA fragments were ligated by adding T4 PNK and T4 ligase. Then, the circularized PCR products were transformed into *E. coli* DH5α to select the correct clones. When cultivating sRNA harboring cells for cloning purposes, the cells were cultivated at 25°C in the presence of 1% arabinose to block sRNA expression (7).

Next, synthetic sRNA vectors harboring two sRNA cassettes were constructed for simultaneous knockdown of two genes. For the construction of double knockdown sRNA

vectors for resveratrol production, insert sRNA fragments were amplified using the primers sRNAdouble_F_1 and sRNAdouble_R_1, which were inserted into sRNA vectors linearized by inverse PCR using the primers sRNAdouble_IV_F_1 and sRNAdouble_IV_R_1 (by Gibson assembly). For the construction of double knockdown sRNA vectors for naringenin production, insertion sRNA fragments were amplified using the primers sRNAdouble_F and sRNAdouble_R, which were inserted into sRNA vectors linearized by inverse PCR using the primers sRNAdouble_IV_F and sRNAdouble_IV_R (by Gibson assembly).

Strains, media and culture conditions. The bacterial and fungal strains used for the sources of heterologous genes, *Streptomyces griseus* subsp. *griseus*, *Saccharopolyspora erythraea*, *Streptomyces peucetius* subsp. *caesius*, *Streptomyces aculeolatus*, *Bacillus subtilis* and *Penicillium griseofulvum* were provided from KCTC (Jeongeup, Republic of Korea). *Streptomyces coelicolor* and *Streptomyces avermitilis* were provided from ATCC (Manassas, VA). For genomic DNA extraction from these strains, the strains were cultivated from the suggested medium listed in ATCC. DNA extraction was performed by using the kit purchased from GeneAll (Seoul, Republic of Korea). For cloning the genes *At4CL1*, *At4CL3*, *At4CL4* and *AtCHI*, the cDNA of the leaves of *Arabidopsis thaliana* was extracted according to the instruction of the kit purchased from GeneAll. Other heterologous genes – *RpALS, AaPKS3, VvSTS* and *PhCHS* – were artificially synthesized as gBlock Gene Fragments from Integrated DNA Technologies Inc. (Skokie, IL). *VvSTS* was codon optimized according to the service provided by the Integrated DNA Technologies Inc. (url: https://sg.idtdna.com/CodonOpt).

For shake flask cultivation of 6MSA, resveratrol and naringenin producers, modified R/2 medium supplemented with 20 g/L glycerol was used. The modified R/2 medium (pH 6.8) contains the followings per liter: 3 g yeast extract, 6.75 g KH_2PO4, 2 g $(NH_4)_2HPO_4$, 0.8 g $MgSO_4 \cdot 7H_2O$, 3 g $(NH_4)_2SO_4$, 0.85 g citric acid and 5 mL trace metal solution (TMS). For shake flask cultivation of aloesone producers, modified R/2 medium supplemented with 20 g/L

glucose was used. Glycerol, glucose, yeast extract, $(NH_4)_2SO_4$, $MgSO_4 \cdot 7H_2O$ and TMS were sterilized separately. The TMS contains the followings per liter of 0.1M HCl: 10 g $FeSO_4 \cdot 7H_2O$, 2.25 g $ZnSO_4 \cdot 7H_2O$, 0.58 g $MnSO_4 \cdot 5H_2O$, 1 g $CuSO_4 \cdot 5H_2O$, 0.1 g $(NH_4)_6Mo_7O_{24} \cdot 4H_2O$, 0.02 g $Na_2B_4O_7 \cdot 10H_2O$, 2 g $CaCl_2 \cdot 2H_2O$ (8). Cells were inoculated from colonies on LB agar plates into 25 mL test tubes containing 10 mL LB medium supplemented with appropriate antibiotics, and were cultivated in a rotary shaker at 200 rpm, 37°C overnight. Then, 1 mL aliquot of each seed culture was transferred into baffled flasks containing 50 mL modified R/2 medium, and were cultivated in a rotary shaker at 37°C, 200 rpm. When the cells grew up to OD_{600} of around 0.8, the cell culture was induced with 0.5 mM isopropyl β-D-1-thiogalactopyranoside (IPTG) and was transferred to another rotary shaker at 30°C, 200 rpm. The cells were cultivated for 48 hours after induction. In *p*-coumaric acid feeding experiments for resveratrol production, 2 mM of *p*-coumaric acid was fed to the medium at the onset of IPTG induction. For the initial RppA expression studies, M9 minimal medium was used; *E. coli* BL21(DE3) was utilized as a host strain unless noted otherwise. The M9 medium contains the followings per liter: 12.8 g $Na_2HPO_4 \cdot 7H_2O$, 3 g KH_2PO_4, 0.5 g NaCl, 1 g NH_4Cl, 2 mM $MgSO_4$, 0.1 mM $CaCl_2$.

Fed-batch fermentation of 6MSA producers was conducted in a 5 L jar fermenter (Marado-PDA, CNS, Daejeon, Republic of Korea) containing 1.9 L of modified R/2 medium supplemented with 100 g/L glycerol. First, a colony of the strain was inoculated into a 25 mL test tube containing 10 mL LB medium supplemented with appropriate concentrations of antibiotics and was cultivated in a rotary shaker at 200 rpm, 37°C overnight. Then, two 250 mL baffled flasks, each containing 50 mL of the modified R/2 medium supplemented with 100 g/L of glycerol, 5.25 g/L 3-(N-morpholino)propanesulfonic acid (MOPS) and appropriate concentrations of antibiotics, were each inoculated with 1 mL aliquot of the seed culture. The cells were cultured (about 9 hours) until the OD_{600} reached around 4, and were inoculated into the fermenter. The culture pH was controlled at 6.8 by automatic feeding of 28% (v/v) ammonia

solution. The dissolved oxygen concentration was controlled at 40% of air saturation by supplying air at 2 L/min and automatically increasing the agitation speed up to 1000 rpm and by changing the percentage of pure oxygen added. The pH-stat feeding strategy was employed in order to supply exhausted nutrients to the fermenter. The feeding solution contains the followings per liter: 800 g glycerol, 6 mL TMS and 12 g $MgSO_4 \cdot 7H_2O$. When the pH becomes higher than 6.86 due to carbon source exhaustion, the feeding solution was automatically added. Heterologous enzyme expression was induced with 0.5 mM of IPTG when the OD_{600} was around 2~3.

Flaviolin production from *P. putida* and *C. glutamicum*. To test flaviolin production in *P. putida* KT2440, the vectors pBBR1-rppA and pBBR1-His-rppA were each introduced into *P. putida*. To test flaviolin production in *C. glutamicum* ATCC 13032, the vectors pCES-rppA and pCES-His-rppA were each introduced into the strain. The colonies of the resultant strains were inoculated to 25 mL test tubes containing 5 mL LB medium supplemented with appropriate concentrations of antibiotics. After 18 hours of cultivation at 30°C, 220 rpm, the cells were transferred to 25 mL test tubes containing 5 mL LB medium supplemented with appropriate concentrations of antibiotics (and with 0.8 g/L $MgSO_4 \cdot 7H_2O$ and 10 g/L glucose for *P. putida*). For *P. putida*, the strains were cultivated for 24 hours; for *C. glutamicum*, the strains were cultivated for 48 hours.

Malonyl-CoA biosensor characterization. For RppA biosensor characterization, the strains *E. coli* BL21(DE3) harboring pTac-5'UTR-Sgr_rppA, *P. putida* KT2440 harboring pBBR1-rppA and *C. glutamicum* ATCC 13032 harboring pCES-His-rppA were used as the sensor strains. For characterizing other type III PKSs AaOKS, AaPKS4 and AaPKS5, the strains *E. coli* BL21(DE3) harboring pET-AaOKS, pET-AaPKS4 and pET-AaPKS5 were used, respectively. The strains were first inoculated to 14 mL disposable Falcon round-bottom tubes (Corning, New York), each containing 3 mL of LB medium supplemented with appropriate

concentrations of antibiotics. For *E. coli*, after 16 hours of cultivation in a rotary shaker at 30°C, 220 rpm, 60 μL of the seed culture was inoculated to 14 mL disposable Falcon round-bottom tubes containing 3 mL of M9 medium supplemented with 10 g/L glucose, 100 μg/mL spectinomycin, 0.2 mM IPTG and appropriate concentrations of cerulenin when necessary. For *P. putida*, after 18 hours of cultivation in a rotary shaker at 30°C, 220 rpm, 40 μL of the seed culture was inoculated to 14 mL disposable Falcon round-bottom tubes containing 2 mL of MR-MOPS medium supplemented with 20 g/L glucose, 25 μg/mL kanamycin, 0.5 mM IPTG and appropriate concentrations of cerulenin when necessary. The MR-MOPS medium (pH 7.0) contains the followings per liter: 6.67 g KH_2PO_4, 4 g $(NH_4)_2HPO_4$, 0.8 g citric acid, 5 mL TMS, 20.09 g MOPS and 0.8 g/L $MgSO_4 \cdot 7H_2O$. For *C. glutamicum*, after 18 hours of cultivation in a rotary shaker at 30°C, 220 rpm, 40 μL of the seed culture was inoculated to 14 mL disposable Falcon round-bottom tubes containing 2 mL of CGXII medium supplemented with 20 g/L glucose, 5 μg/mL biotin, 12.5 μg/mL thiamine·HCl, 25 μg/mL kanamycin, 0.5 mM IPTG and appropriate concentrations of cerulenin when necessary. Cerulenin and IPTG was added when OD_{600} was around 2 to avoid reduced cell viability by cerulenin. The CGXII medium (pH 7.0) contains the followings per liter: 20 g $(NH_4)_2SO_4$, 5 g urea, 1 g KH_2PO_4, 1 g K_2HPO_4, 42 g MOPS, 30 mg protocatechuic acid, 0.5 g $MgSO_4 \cdot 7H_2O$ and 5 mL TMS. The TMS used for *C. glutamicum* contains the followings per liter: 2.6 g $CaCl_2 \cdot 2H_2O$, 2.0 g $FeSO_4 \cdot 7H_2O$, 2.8 g $MnSO_4 \cdot 5H_2O$, 0.2 g $ZnSO_4 \cdot 7H_2O$, 0.06 g $CuSO_4 \cdot 5H_2O$, 4 mg $NiCl_2 \cdot 6H_2O$ and 10 mL HCl (35%). For testing different intracellular malonyl-CoA levels, cerulenin titration was performed since cerulenin addition increases intracellular malonyl-CoA concentration by inhibiting fatty acid biosynthesis. Cerulenin concentration tested: 0, 5, 10, 15, 20, 25, 50, 100 μM. Since the growth of *C. glutamicum* was severely retarded when cerulenin was added above 15 μM, cerulenin concentrations tested for *C. glutamicum* were 0, 5, 10, 15 μM. For the PKSs AaOKS, AaPKS4 and AaPKS5, cerulenin concentrations of up to 50 μM were used. After

inoculation, the cells were incubated in a rotary shaker at 30°C, 220 rpm for 16 hours (*E. coli*), 12 hours (*P. putida*) or 20 hours (*C. glutamicum*). Then, the cells were centrifuged for 20 minutes at 4,000 ×*g*, and 150 μL of each supernatant was transferred to a 96-well transparent flat-bottomed microplate (SPL Life Sciences; Pocheon, Republic of Korea) to measure its optical density at 340 nm (for AaOKS, AaPKS4 and AaPKS5, 300 nm) using a microplate reader (SpectraMax M2; Molecular Devices, San Jose, CA). In addition, the cell pellets were resuspended in phosphate buffered saline (PBS) to measure cell growth (OD_{600}) using the microplate reader. The biosensor signal was defined as OD_{340} of the supernatant for RppA and OD_{300} of the supernatant for AaOKS, AaPKS4 and AaPKS5. For characterizing the biosensor, normalized signal (divided by OD_{600} of the cell) was used.

High-throughput screening of malonyl-CoA overproducers. The constructed *E. coli* genome-scale synthetic sRNA library was transformed into the sensor strain (*E. coli* BL21(DE3) harboring pTac-5'UTR-Sgr_rppA) and spread onto 150 mm plates (SPL Life Sciences) containing LB agar supplemented with 100 μg/mL of spectinomycin and 100 μg/mL of ampicillin. As described in Fig. S5*A*, we concluded that we could cover all 1,858 sRNAs by selecting colonies of >6-fold of the library size. Therefore, 11,488 colonies were inoculated to 96-well transparent flat-bottomed microplates (SPL Life Sciences), with each well containing 150 μL of LB medium supplemented with appropriate concentrations of antibiotics and 0.2 mM IPTG. For robotic high-throughput screening, automatic K3 colony picker (KBiosystems, Basildon, UK) was employed (Korea Research Institute of Bioscience and Biotechnology (KRIBB); Jeongeup, Republic of Korea) for transferring colonies to liquid medium (9). The K3 colony picker (KBiosystems) illuminates and images the agar plates. Then, the intrinsic program recognizes and locates colonies and instruct a robot arm tipped with pins to pick the selected colonies. After inoculation, the pins are sterillized in ethanol or peroxide, heated and dried. The cells were then cultivated in HT-MegaGrow shaking incubator (Bioneer, Daejeon,

Republic of Korea) at 30°C, 500 rpm for 24 hours. Then, 231 strains with increased signals were selected and were cultivated again in 14 mL disposable Falcon round-bottom tubes containing 3 mL of LB medium supplemented with appropriate concentrations of antibiotics and 0.2 mM IPTG to verify the results. 70 strains with true-positive hits were sequenced to identify the synthetic sRNAs introduced. Among them, 26 knockdown gene targets showing more than 45% increase in the signal were put to test by individually transforming the corresponding sRNA vectors back into the native sensor strain (*E. coli* BL21(DE3) harboring pTac-5'UTR-Sgr_rppA). The transformed cells were cultivated in 14 mL disposable Falcon round-bottom tubes containing 3 mL of LB medium in the same manner as described above. The biosensor signals were measured by OD_{340} of culture supernatant. The final sRNA targets were selected according to the set threshold of >70% increase in sensor signal relative to that of the control strain (without sRNA).

Test tube scale cultivation. For test tube scale cultivation of flaviolin, 6MSA and aloesone producers, each colony was first inoculated into 14 mL disposable Falcon round-bottom tube containing 3 mL of LB supplied with appropriate concentrations of antibiotics. After 16 hours of cultivation in a rotary shaker at 37°C, 200 rpm, the cells were transferred to a different rotary shaker at 30°C, 220 rpm where 60 μL of the seed culture was used to inoculate 3 mL of modified R/2 medium. Here, 0.5 mM IPTG, appropriate concentrations of antibiotics, and 100 g/L glycerol for 6MSA or 20 g/L glucose for flaviolin and aloesone were supplied. The cells were cultivated for 24 hours for flaviolin and 48 hours for 6MSA and aloesone. After cultivation, the cells were centrifuged for 15 minutes at 4,000 ×*g* before filtration with 0.22 μm PVDF syringe filters (FUTECS, Daejeon, Republic of Korea) for HPLC analysis.

Malonyl-CoA quantification. For intracellular malonyl-CoA quantification, *E. coli* cells were cultivated in the same manner as in the "**RppA malonyl-CoA biosensor characterization**" section above. *E. coli* BL21(DE3) harboring pTacCDFS was first inoculated to 14 mL

disposable Falcon round-bottom tubes (Corning, New York), each containing 3 mL of LB medium supplemented with appropriate concentrations of antibiotics. After 16 hours of cultivation in a rotary shaker at 30°C, 220 rpm, 60 μL of the seed culture was inoculated to 14 mL disposable Falcon round-bottom tubes containing 3 mL of M9 medum supplemented with 10 g/L glucose, 100 μg/mL spectinomycin, 0.2 mM IPTG and appropriate concentrations of cerulenin when necessary: 0, 5, 10, 15, 20, 25, 50, 100 μM. After inoculation, the cells were incubated in a rotary shaker at 30°C, 220 rpm for 16 hours. Cell growth was measured by measuring absorbance at 600 nm (OD_{600}) using Ultrospec 3100 spectrophotometer (Amersham Biosciences, Uppsala, Sweden). Cell concentration defined as gram dry cell weight (gDCW) per liter was calculated from the predetermined standard curve (1 OD_{600} = 0.52 gDCW/L). For malonyl-CoA quantification, analytical samples were prepared as previously reported (10, 11); 2.6 mL of each cell culture was chilled in ice and centrifuged at 4,000 ×*g* and 4°C for 10 min. Pellets were washed in 1 mL PBS and centrifuged at 10,000 ×*g* and 4°C for 1 min. Cell lysis, quenching and metabolite extraction was performed by adding 150 μL of lysis buffer (45:45:10 acetonitrile/methanol/H2O + 0.1% glacial acetic acid) in ice and vigorously vortexing. The extract was incubated in ice for 15 min with intermittent vortexing. After 15 min, ammonium hydroxide was added to neutralize the previously incorporated acetic acid, and each extract was centrifuged for 3 min at 15,000 ×*g* and 4°C. The supernatant was subjected to LC-MS analysis.

Analytical procedures. Cell growth was monitored by measuring the absorbance at 600 nm (OD_{600}) with an Ultrospec 3100 spectrophotometer (Amersham Biosciences, Uppsala, Sweden). The concentration of glucose, glycerol and acetic acid were measured using HPLC (1515 isocratic pump, Waters) equipped with refractive index detector (2414, Waters). A MetaCarb 87H column (Agilent) was used and the mobile phase (0.01 N H_2SO_4) was flown at 0.5 mL/min. The column was operated at 25 ^{o}C. For the analysis of flaviolin, 6MSA and

aloesone, culture supernatant was filtrated through 0.22 μm PVDF syringe filters (FUTECS). For the analysis of naringenin and resveratrol, culture supernatant was extracted with an equal volume of ethyl acetate, dried and resolubilized in methanol. The prepared samples were analyzed with high-performance liquid chromatography (HPLC; 1260 Infinity II; Agilent Technologies, Palo Alto, CA) equipped with DAD detectors (G7115A; Agilent) and C18 columns (4.6 × 150 mm; Agilent). For the analysis of 6MSA, the mobile phase was run at 25°C at a flow rate of 0.8 mL/min; the mobile phase consists of solvent A (0.1% formic acid) and solvent B (methanol). The following gradient was applied: 0-1 min, 30% solvent B; 1-15 min, a linear gradient of solvent B from 30% to 70%; 15-20 min, a linear gradient of solvent B from 70% to 90%; 20-24 min, 90% solvent B; 24-25 min, a linear gradient of solvent B from 90% to 30%. For the analysis of aloesone, the mobile phase was run at 25°C at a flow rate of 0.4 mL/min; the mobile phase consists of solvent A (0.1% formic acid) and solvent B (methanol). The following gradient was applied: 0-1 min, 5% solvent B; 1-15 min, a linear gradient of solvent B from 5% to 70%; 15-20 min, a linear gradient of solvent B from 70% to 100%; 20-25 min, 100% solvent B; 25-26 min, a linear gradient of solvent B from 100% to 5%. For the analysis of resveratrol, the mobile phase was run at 30°C at a flow rate of 1.0 mL/min; the mobile phase consists of solvent A (0.1% formic acid) and solvent B (acetonitrile). The following gradient was applied: 0-3 min, 10% solvent B; 3-10 min, a linear gradient of solvent B from 10% to 100%; 10-15 min, 100% solvent B. For the analysis of naringenin, the mobile phase was run at 30°C at a flow rate of 0.8 mL/min; the mobile phase consists of solvent A (0.1% trifluoroacetic acid) and solvent B (acetonitrile). The following gradient was applied: 0-3 min, 5% solvent B; 3-20 min, a linear gradient of solvent B from 5% to 70%; 20-25 min, 70% solvent B (all in vol%). Samples were monitored at 254 nm for flaviolin, 306 nm for 6MSA, 300 nm for aloesone, 305 nm for resveratrol and 330 nm for naringenin. Since commercial flaviolin and aloesone standards were unavailable, they were purified via fraction collector

(G1364C; Agilent) attached to the HPLC. The purified chemicals were used as authentic standard chemicals.

The produced natural products (flaviolin, 6MSA, aloesone, resveratrol, naringenin) were further analyzed by HPLC (1100 Series HPLC; Agilent) connected with MS (LC/MSD VL; Agilent), and by comparing with the LC-MS spectrum of the commercially available authentic standards. A C18 column (4.6 × 150 mm; Agilent) was used and operated at 25^{o}C. Two mobile phase solvents were used: solvent A (0.1% formic acid) and solvent B (0.1% formic acid in methanol). For the analysis of flaviolin, 6MSA, resveratrol and naringenin, the total flow rate was maintained at 0.4 mL/min, and the following gradient was applied: 0-1 min, 30% solvent B; 1-10 min, a linear gradient of solvent B from 30% to 70%; 10-30 min, a linear gradient of solvent B from 70% to 95%; 30-31 min, a linear gradient of solvent B from 95% to 100% (all in vol%). The eluent was continuously injected into the mass spectrometer using electrospray ionization (ESI) negative ion mode with following conditions: fragmentor, 120V; drying gas flow, 12.0 L/min; drying gas temperature, 350 ^{o}C; nebulizer pressure, 30 psig; capillary voltage, 2.5 kV. For analysis, scan mode was used and the scanned mass range was *m/z* of 100-400. For the analysis of aloesone, the total flow rate was maintained at 0.4 mL/min, and the following gradient was applied: 0-1 min, 30% solvent B; 1-10 min, a linear gradient of solvent B from 30% to 70%; 10-30 min, a linear gradient of solvent B from 70% to 95%; 30-31 min, a linear gradient of solvent B from 95% to 100%; 31-35 min, 100% solvent B (all in vol%). The eluent was continuously injected into the mass spectrometer using electrospray ionization (ESI) positive ion mode with following conditions: fragmentor, 120V; drying gas flow, 12.0 L/min; drying gas temperature, 350 ^{o}C; nebulizer pressure, 30 psig; capillary voltage, 2.5 kV. For analysis, scan mode was used and the scanned mass range was *m/z* of 200-300.

The produced natural compounds without authentic commercial standards (flaviolin, aloesone) were further analyzed by tandem mass spectrometry (KAIST Analysis Center for

Research Advancement (KARA); Daejeon, Republic of Korea). The samples were injected into the tandem mass spectrometry (micrOTOF-QII; Bruker, Billerica, MA) using ESI negative ion mode with following conditions: drying gas flow, 3.5 L/min; drying gas temperature, 180 ºC; nebulizer pressure, 0.5 bar; capillary voltage, 3.2 kV. For flaviolin: collision cell RF, 150 Vpp; collision energy, 15 eV. Selected ion was *m/z* of 205; scanned mass range was *m/z* of 50-600. For the analysis of aloesone, ESI positive ion mode was used; collision cell RF, 180 Vpp; collision energy, 10 eV. Selected ion was *m/z* of 233; scanned mass range was *m/z* of 50-700.

For malonyl-CoA quantification, LC-MS was employed by comparing with the LC-MS spectrum of the commercially available authentic malonyl-CoA standard. A C18 column (4.6 × 150 mm; Agilent) was used and operated at 25 ºC. Two mobile phase solvents were used: solvent A (10 mM tributylamine, 15 mM acetic acid and 5% methanol in distilled water) and solvent B (isopropyl alcohol). The initial total flow rate was 0.8 mL/min, and the following gradient was applied: 0-0.5 min, 100% solvent A (flow 0.8 mL/min); 0.5-1.5 min, a linear gradient of solvent B from 0% to 12% (flow 0.8 mL/min); 1.5-10 min, a linear gradient of solvent B from 12% to 27.5% (flow 0.5 mL/min); 10-20 min, a linear gradient of solvent B from 27.5% to 90% (flow 0.3 mL/min); 20-25 min, 90% solvent B (flow 0.3 mL/min); 25-28 min, a linear gradient of solvent B from 90% to 0% (flow 0.3 mL/min); 28-35 min, 100% solvent A (flow 0.8 mL/min; all in vol%). Samples were monitored by DAD detectors at 260 nm. The eluent was continuously injected into the mass spectrometry using electrospray ionization (ESI) negative ion mode with following conditions: fragmentor, 240V; drying gas flow, 12.0 L/min; drying gas temperature, 350 ºC; nebulizer pressure, 35 psig; capillary voltage, 2.5 kV. For analysis, scan mode was used and the scanned mass range was *m/z* of 700-1000.

Genome engineering. We constructed the *E. coli* BAP1 strain, a chassis strain for polyketide production derived from *E. coli* BL21(DE3), according to a previous report (12). For polyketide chain elongation, 4'-phosphopentatheinylase (encoded by *sfp*) from *Bacilus subtilis*

is needed to activate acyl-carrier protein (ACP) in its active holo form from inactive apo form. Also, in *E. coli* BAP1 strain, propionate catabolism associated *prpRBCD* operon was knocked out and *prpE*, which encodes propionyl-CoA ligase, is overexpressed by changing the promoter to the strong *T7* promoter. Exchanging the genetic parts within the *E. coli* genome was carried out using a one-step inactivation method as previously reported (13, 14).

***In silico* analysis.** To identify amplification gene targets for the enhanced malonyl-CoA production, *in silico* analysis was performed using the *E. coli* genome-scale metabolic model iJO1366 (15). The FVSEOF algorithm was used to grasp the tendency of metabolic flux changes of intracellular reactions while gradually increasing the malonyl-CoA production rate (16). Also, flux response analysis was performed to examine the effects of two carbon sources, glucose and glycerol, on the production of malonyl-CoA. The malonyl-CoA production rate was maximized as the growth rate was gradually increased from minimum to maximum values. The glucose and glycerol uptake rate was set to 10 mmol/gDCW/hr and 20 mmol/gDCW/hr, respectively, considering its carbon number (C3 for glycerol, C6 for glucose). All simulations were conducted in Python environment with Gurobi Optimizer 6.0 and GurobiPy package (Gurobi Optimization, Inc., Houston, TX). Reading, writing and manipulation of the COBRA-compliant SBML files were implemented using COBRApy (17).

SDS-PAGE analysis. In order to confirm the expression of heterologous enzymes including Pg6MSAS, Sfp, At4CL1m, At4CL3, At4CL4, Sc4CLm, VvSTS, RsTAL, AtCHI, AtCHS, RpALS and AaPKS3, *E. coli* BL21(DE3) strains harboring the respective recombinant plasmids were collected (3 mL of cells when their OD_{600} reached 1.0) from the 10 mL modified R/2 medium culture supplemented with either 10 g/L of glycerol or glucose. The cells were grown at 30°C and were induced with 0.5 mM IPTG when the OD_{600} of the cells were between 0.4 to 0.6. Cell pellets were washed with 1 mL of cold PBS solution (pH 7.4), centrifuged at 15,000 ×*g* for 1 min at 4°C and resuspended in 0.3 mL of the same buffer. The resuspended

cells were lysed by sonication (High-Intensity Ultrasonic Liquid Processors, Sonics & Materials Inc., Newtown, CT). In order to precipitate insoluble protein fractions and partially disrupted cells, the sonicated samples were centrifuged at 15,000 ×*g* for 10 min at 4°C. Crude cell lysates were used for total protein expression analysis and the supernatants were used for soluble protein expression analysis.

Statistical analysis. We did not predetermine sample sizes. All colonies were randomly selected from plates containing 100–200 colonies and subject to independent flask culture and chemical analysis. All numerical data are presented as mean ± SD (standard deviation) from experiments done in triplicate. Means were compared using a two-tailed Student's *t*-test. *P* values were represented $*P < 0.05$, $**P < 0.01$ or $***P < 0.001$, which were considered as significant. The investigators were blinded to the group allocation by randomly selecting single colonies multiple times.

SI Appendix Texts

Text S1. THN can be spontaneously converted to flaviolin by a non-enzymatic oxidation reaction.

RppA is responsible for the conversion of five molecules of malonyl-CoA to THN (18). Whereas the subsequent conversion of THN to flaviolin is a spontaneous non-enzymatic oxidation reaction, it was also reported that a number of monooxygenases are responsible for the conversion of THN to flaviolin in *Streptomyces* species (19). Therefore, we isolated a well characterized monooxygenase, WhiE-ORFII from *Streptomyces coelicolor*, and cloned the gene into the pET-Sgr_rppA plasmid to construct pET-Sgr_rppA_whiE. *E. coli* BL21(DE3) harboring pET-Sgr_rppA and *E. coli* BL21(DE3) harboring pET-Sgr_rppA_whiE were cultivated in shake flasks containing 50 mL of M9 medium supplemented with 10 g/L glucose and appropriate concentrations of antibiotics. Notably, flaviolin production decreased when WhiE_ORFII was coexpressed with RppA; we speculated that the *whiE*_ORFII gene inserted at the downstream of *rppA* in a single operon negatively affected *rppA* expression. Nevertheless, it was thus concluded that *rppA* alone is sufficient for the production of flaviolin in *E. coli*, as was also reported in previous studies (20-22).

Text S2. Selection of knockdown gene targets for *E. coli* genome-scale synthetic sRNA library construction.

First, 1,027 major metabolic genes were selected from *E. coli* K-12 W3110 strain according to the previously reported *E. coli in silico* model iJO1366 (15). This model included 1,366 genes corresponding to 2,251 metabolic reactions. Also included in the list were 611 essential genes as was previously reported (23). These essential genes cannot be eliminated from the genome, thus requires sRNA-based knockdown in order to be downregulated. In addition, 210 genes encoding transcription factors were selected from the RegulonDB, the database containing *E. coli* regulatory gene circuits; transcription factors are worthwhile to examine since a single transcription factor is responsible for the expression of many related genes. Ten sigma or anti-sigma factors were also included in the library list (24).

Text S3. Effects of overexpressing FVSEOF gene targets on malonyl-CoA accumulation.

To assess amplification gene targets, the FVSEOF algorithm was utilized for the identification of potential overexpression gene targets beneficial for increased malonyl-CoA flux. The FVSEOF algorithm scans the changes in metabolic flux variabilities in response to an enforced flux toward a target chemical (16). The effects of the selected targets (*zwf*, *mdh*, *fumA*, *fumB*, *fumC*, *serA*, *serB*, *serC* and *tpiA*) on intracellular malonyl-CoA concentration were tested by employing the RppA malonyl-CoA biosensor (Fig. S7*A* and *C*). Each of the nine genes from *E. coli* BL21(DE3) was cloned into pTrc99A and was introduced into the sensor strain. The resulting strains were cultivated for 24 hours at 30°C in 14 mL round-bottom tubes containing 3 ml of LB medium supplemented with 0.2 mM IPTG and appropriate concentrations of antibiotics, in order to measure the signals. Among the nine screened overexpression gene targets, eight gene targets showed increased signal compared to that of the control strain without gene overexpression (Fig. S7*B*).

Text S4. Enhanced polyketide production by metabolic engineering.

For 6MSA production, pTac-Pg6MSAS-sfp was constructed and introduced into *E. coli* BL21(DE3). However, since Pg6MSAS is encoded by a long DNA sequence (5.3 kb), we speculated that expressing the gene alone in a plasmid might aid in its expression with regard to gene expression and plasmid stability issues. Therefore, to further enhance 6MSA production, different genetic constructs were tested to optimize expression of *Pg6MSAS* and *sfp* (Fig. S8*A* and *B*). When the *sfp* gene was expressed from the chromosome (*E. coli* BAP1 strain; 12) while the *Pg6MSAS* gene from a plasmid (pTac-Pg6MSAS), 17.6 mg/L of 6MSA was produced (Fig. S9*A*). This was found, by SDS-PAGE, to be due to enhanced Sfp expression along with enhanced solubility of Pg6MSAS by this new genetic construct (Fig. S8*C*). When the anti-*pabA* sRNA was additionally expressed in the *E. coli* BAP1 strain harboring pTac-Pg6MSAS, 6MSA production was further increased to 23.9 mg/L which corresponds to 35.8% increase than that obtained without sRNA expression (Fig. S9*E*). For further enhancement in 6MSA titer, the strain was overexpressed with either of the three FVSEOF gene targets showing significant ($P < 0.05$) increase in RppA signal (*zwf*, *mdh*, *serA*; Fig. S7*B*). In addition, five enzyme targets (acetyl-CoA carboxylase from *C. glutamicum* encoded by *accBC* and *accD1*, glyceraldehyde-3-phosphate dehydrogenase from *E. coli* BL21 encoded by *gapA*, phosphoglycerate kinase from *E. coli* BL21 encoded by *pgk*, acetyl-CoA synthetase from *E. coli* encoded by *acs* and pyruvate dehydrogenase from *E. coli* BL21 encoded by *aceEF* and *lpd*) were rationally selected and individually overexpressed to increase malonyl-CoA pool (25, 26). After flask cultivation of the eight resultant strains, the strain overexpressed with *C. glutamicum accBCD1* showed the highest 6MSA titer of 63.6 mg/L (Fig. S9*F*). Fed-batch fermentation of this strain produced 440.3 ± 30.2 mg/L of 6MSA in 58 hours (Fig. 4*D*).

Combinatorial knockdown of target genes screened using the RppA biosensor could also increase aloesone titer. When the anti-*pabA* sRNA was additionally expressed in *E. coli*

BL21(DE3) harboring pCDF-RpALS, aloesone production was increased to 27.1 mg/L which corresponds to 32.2% increase than that obtained without sRNA expression (Fig. S10*D*). For further enhancement in aloesone titer, the strain was additionally overexpressed with eight enzyme targets as was tested for 6MSA production described above (each encoded by *zwf, mdh, serA, accBCD1, gapA, pgk, acs* and *aceEF-lpd*). After flask cultivation of the eight resultant strains, the strain overexpressed with *zwf* showed the highest aloesone titer of 30.9 mg/L (Fig. S10*E*).

Text S5. Construction of the heterologous resveratrol biosynthetic pathway.

For the conversion of *p*-coumaric acid to *p*-coumaroyl-CoA, different 4-coumarate:CoA ligases from *Arabidopsis thaliana* (At4CL) and *S. coelicolor* (Sc4CL) were tested: At4CL1 mutant (At4CL1m; I250L/N404K/I461V) (27), At4CL3 (28), At4CL4 (28) and Sc4CL mutant (Sc4CLm; A294G/A318G) (29). As previously reported, At4CL1m and Sc4CLm were mutated to allow higher affinity towards *p*-coumaric acid (27, 29). Then, for the subsequent conversion of *p*-coumaroyl-CoA into resveratrol by the condensation of *p*-coumaroyl-CoA with 3 molecules of malonyl-CoA, stilbene synthase from *Vitis vinifera* (VvSTS) was employed (Fig. S11) (30). First, each of these genes was introduced into pTac15K, and expression of all the enzymes was confirmed by SDS-PAGE (Fig. S12*A*). Then, either of the genes encoding the four 4CLs was assembled with *VvSTS* to construct the plasmids pTac-VvSTS-At4CL1m, pTac-VvSTS-At4CL3, pTac-VvSTS-At4CL4 and pTac-VvSTS-Sc4CLm in polycistronic configurations. Resveratrol production from the *E. coli* BL21(DE3) strains introduced with these vectors was compared by shake flask cultivation supplemented with 20 g/L of glycerol and 2 mM of *p*-coumaric acid. Among these strains, *E. coli* BL21(DE3) harboring pTac-VvSTS-At4CL1m showed the highest resveratrol titer of 18.0 mg/L (Fig. S12*B*). The authenticity of the produced resveratrol was confirmed by LC-MS (Fig. S13*A* and *B*). When glucose was used as the carbon source, only 0.2 mg/L of resveratrol was produced from the same strain. Since the conversion from *p*-coumaric acid to resveratrol was low, it was suggested that low malonyl-CoA availability might be the potential bottleneck. Before investigating the effects of increasing malonyl-CoA pool on resveratrol production, we first sought to optimize the activities of the heterologous enzymes, which might be another potential bottleneck. Therefore, additional efforts including expressing the genes in an operon and fusing the two enzymes were conducted. However, these could not further improve resveratrol production (Fig. S12*C*: strains 1-3). We then moved the resveratrol biosynthetic gene cluster in pTac-

VvSTS-At4CL1m to pTacCDFS, a pCDFDuet-1 derivative. This was because both pTY13-HisTAL harboring *p*-coumaric acid biosynthetic pathway and pTac-VvSTS-At4CL1m have the same origin of replication (*Text S6*). The strain harboring the resultant vector pTacCDF-VvSTS-At4CL1m could produce 21.2 mg/L of resveratrol from 2 mM *p*-coumaric acid and 20 g/L glycerol (Fig. S12*C*: strain 4).

Text S6. Construction of a *p*-coumaric acid producing *E. coli* strain.

As the first step for the construction of a *p*-coumaric acid producer, we utilized the previously reported L-tyrosine overproducing *E. coli* strain, BTY5.13 (BTY5 harboring pTY13) (31). Tyrosine ammonia-lyase from *Saccharothrix espanaensis* (SeTAL) is responsible for the conversion of L-tyrosine into *p*-coumaric acid, which was cloned into the pTrc99A plasmid. Then, in order to test different N-terminal tags on SeTAL expression, and thus on *p*-coumaric acid production, poly-His-tag and *E. coli* thioredoxin (encoded by *trxA*) were each attached to the N-terminus of SeTAL. The BTY5.13 strain was additionally introduced with each of pTrc-SeTAL, pTrc-HisTAL and pTrc-TrxTAL. The resultant strains were cultivated in shake flasks containing 50 mL of modified MR medium supplemented with 20 g/L glucose, at 30°C and 200 rpm, for 36 hours after induction with 1 mM IPTG. The modified MR medium contains the followings per liter: 6.67 g KH_2PO_4, 4 g $(NH_4)_2HPO_4$, 0.8 g citric acid, 0.8 g $MgSO_4 \cdot 7H_2O$, 5 mL TMS, 2 g yeast extract and 15 g $(NH_4)_2SO_4$. Since it turned out that N-terminal poly-His-tag attachment was the most effective for *p*-coumaric acid production (412 mg/L), we decided to integrate the P*trc*-HisTAL fragment into the pTY13 vector (Fig. S12*D*). When the strain BTY5 harboring pTY13-HisTAL was cultivated in shake flasks, 0.35 g/L of *p*-coumaric acid was produced from 20 g/L glycerol (Fig. S12*D*).

Text S7. Construction of the heterologous naringenin biosynthetic pathway.

For the conversion of *p*-coumaric acid to *p*-coumaroyl-CoA, At4CL1m was utilized. Then, for the subsequent conversion of *p*-coumaroyl-CoA to naringenin chalcone by incorporation of three molecules of malonyl-CoA, chalcone synthase from *A. thaliana* (AtCHS) was tested. However, since AtCHS turned out to be insoluble in *E. coli* (Fig. S14*A*), we introduced chalcone synthase from *Petunia x hybrida* (PhCHS) instead. We next cloned the gene encoding chalcone isomerase from *A. thaliana* (AtCHI) for the further conversion of naringenin chalcone to naringenin. All three genes were expressed as an operon under the *trc* promoter in the pTrcCDFS plasmid. The constructed pTrcCDF-At4CL1m-AtCHI-PhCHS vector was introduced into *E. coli* BL21(DE3), and expression of all the heterologous enzymes was confirmed by SDS-PAGE analysis (Fig. S14*B*). From glucose and *p*-coumaric acid, 4.8 mg/L of naringenin was produced whereas 6.1 mg/L of naringenin was produced from glycerol and *p*-coumaric acid (Fig. S14*C*). Then, the plasmid pTrcCDF-At4CL1m-AtCHI-PhCHS was introduced into the *p*-coumaric acid producer (BTY5 harboring pTY13-HisTAL). Interestingly, notable increase in naringenin titers for both glucose and glycerol supplementation was observed; 37.2 mg/L of naringenin was produced from glucose and 64.5 mg/L of naringenin was produced from glycerol (Fig. S14*C*). The authenticity of the produced naringenin was confirmed by LC-MS (Fig. S14*D* and *E*).

Text S8. Flux response analysis of the malonyl-CoA flux on different carbon sources.

For 6MSA, resveratrol and naringenin, higher titers were obtained when glycerol was used as carbon source. In order to find the effects of glycerol and glucose on metabolic flux towards malonyl-CoA, *in silico* flux response analysis was performed. Glycerol was found to allow better cell growth and higher malonyl-CoA flux when compared to glucose (Fig. S15*A*). In the cases of resveratrol and naringenin, it has been reported that lower phenylpropanoid production using glucose was due to catabolite repression of the operons *hca* and *mhp*, which are responsible for the transport of phenylpropanoids (32). In addition, glycerol catabolism regenerates two more molecules of NADH (per six carbon equivalent; two glycerol molecules) than glucose, thus is generally considered to be more beneficial for biosynthetic pathways requiring sufficient reducing power. Even when this advantage of additional redox generation was not considered by artificially deleting the NADH generation in glycerol dehydrogenase reaction, *in silico* flux response analysis revealed that glycerol was still slightly better than glucose in terms of cell growth and malonyl-CoA flux (Fig. S15*B*). One mole of NADPH is needed per one mole of 6MSA biosynthesis. Also, it was reported that 6MSAS can also utilize NADH as a reducing agent (33). Thus, increased reducing equivalents generated by using glycerol as a carbon source seems to be beneficial for enhanced 6MSA production. On the other hand, since no reducing power is needed for aloesone production, the beneficial effect of using glycerol was not observed.

SI Appendix Figures

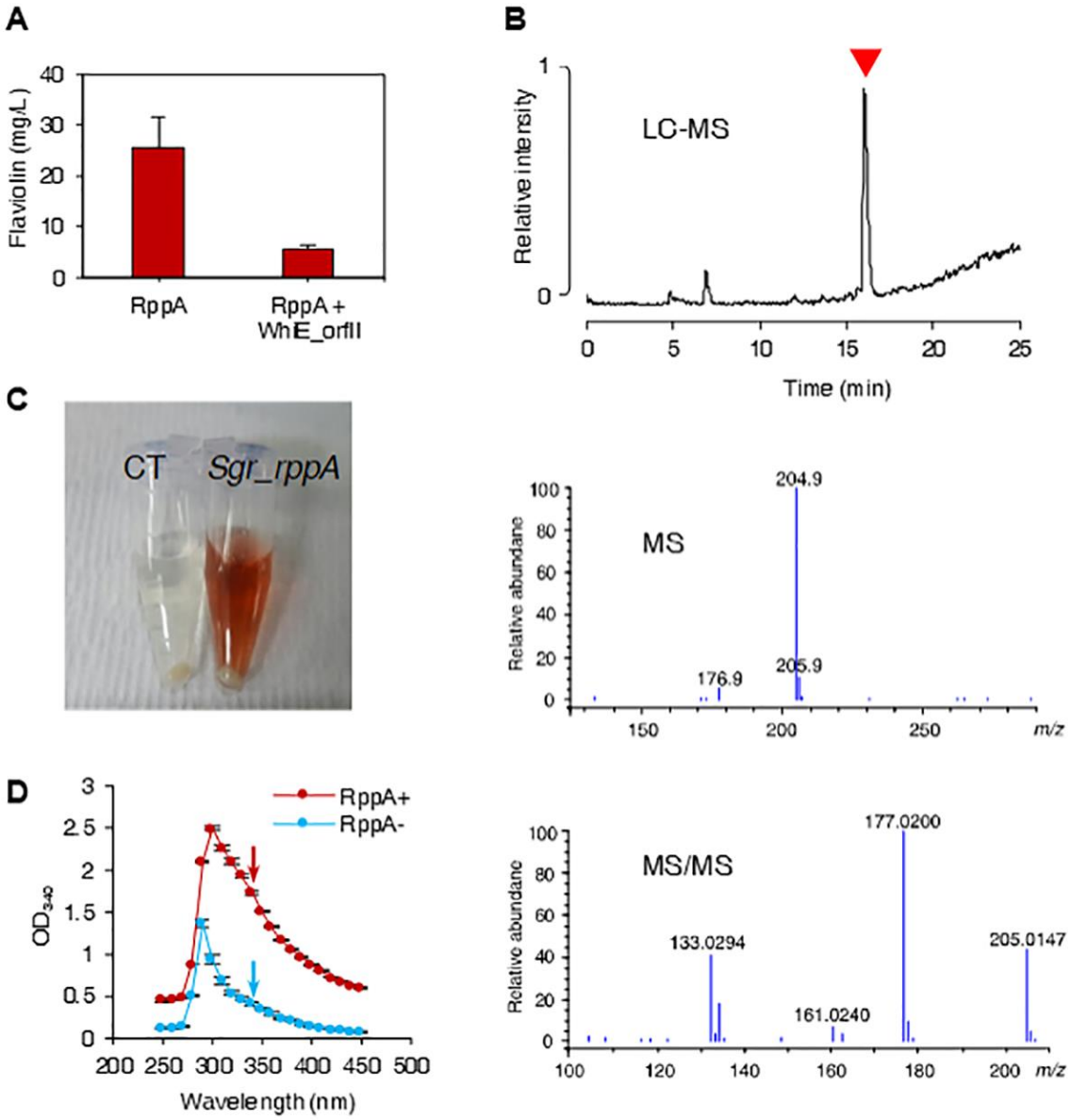

Fig. S1. Characterization of flaviolin produced from an engineered *E. coli*. (*A*) Introduction of *whiE*_ORFII does not aid in flaviolin production as is also described in *Text S1*. Error bars, mean ± SD (n = 2). (*B*) LC-MS chromatogram (R_t 16.0 min), MS spectrum (*m/z* 204.9 $[M-H]^-$) and MS/MS fragmentation pattern (*m/z* 205.0147 $[M-H]^-$, *m/z* 177.0200 $[M-H-CO]^-$, *m/z* 161.0240 $[M-H-CO_2]^-$, *m/z* 133.0294 $[M-H-CO-CO_2]^-$) of flaviolin (34). The molecular weight of flaviolin is 206.153 g/mol. The red arrow denotes the LC-MS flaviolin peak corresponding

to the MS spectrum below. (*C*) Flaviolin is secreted into the medium rather than accumulating inside the *E. coli* cell. CT denotes the control strain without *rppA* expression; *Sgr_rppA* denotes *E. coli* BL21(DE3) harboring pET-Sgr_rppA. (*D*) Absorbance of culture supernatant of *E. coli* DH5α harboring RppA (denoted as RppA+) and the strain without harboring RppA (denoted as RppA-) at different wavelengths. Absorbances at 340 nm are denoted as arrows.

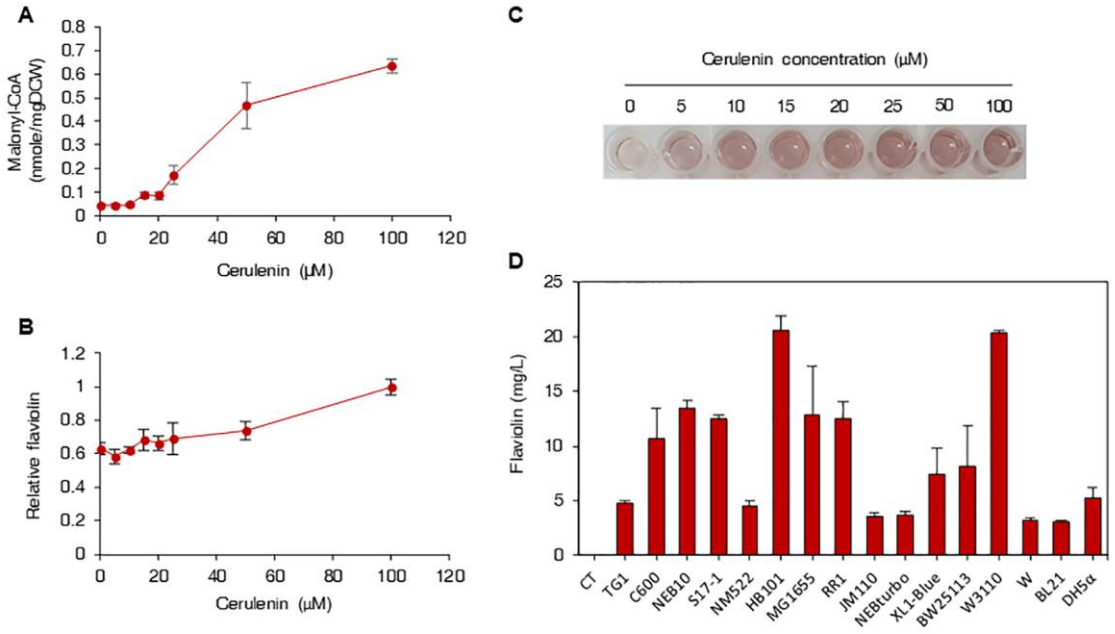

Fig. S2. Intracellular malonyl-CoA titration using cerulenin. (*A*) Intracellular malonyl-CoA concentrations of *E. coli* harboring pTacCDFS according to different concentrations of cerulenin. (*B*) Relative flaviolin production from *E. coli* normalized with cell growth increases with increased cerulenin concentration. The data represents relative flaviolin titers normalized with cell growth (OD_{600}), at the specified cerulenin concentrations. Flaviolin concentration was measured by HPLC. In (*A*) and (*B*), the cells were cultivated in 14 mL disposable Falcon round-bottom tubes containing 3 mL of M9 medium supplemented with 10 g/L glucose, 100 μg/mL spectinomycin, 0.2 mM IPTG and appropriate concentrations of cerulenin when necessary. (*C*) Increased flaviolin production can be easily detected through the naked eyes. (*D*) Flaviolin production from 16 different *E. coli* strains each harboring pTac-5'UTR-Sgr_rppA. The cells were cultivated in 14 mL disposable Falcon round-bottom tubes containing 3 mL of modified R/2 medium supplemented with 0.5 mM IPTG, appropriate concentrations of antibiotics, and 20 g/L glucose. CT, control strain (DH5α harboring pTacCDFS). All error bars, mean ± SD (*n* = 3).

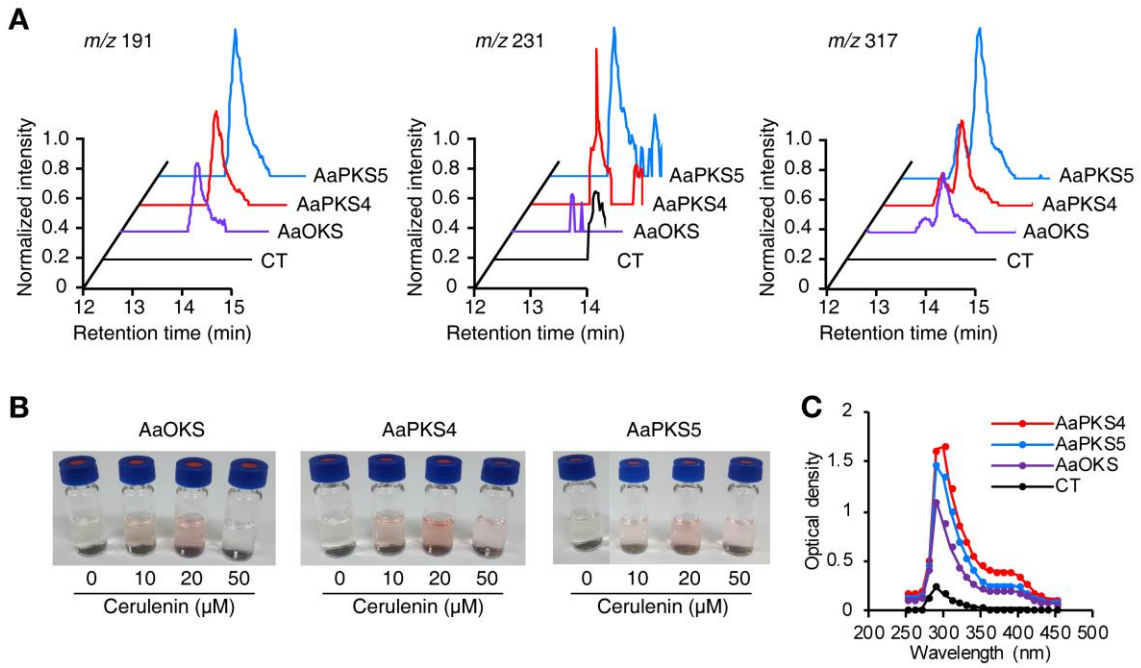

Fig. S3. Characterization of other type III PKSs as malonyl-CoA biosensors. (*A*) Extracted ion chromatograms of culture supernatants of *E. coli* BL21(DE3) strains expressing AaOKS, AaPKS4 and AaPKS5 generated by LC-MS (negative scan mode). CT, control (*E. coli* BL21(DE3) harboring pET-30a(+)). The assumed polyketides produced are as follows (35): 5,7-dihydroxy-2-methylchromone (*m/z* 191); aloesone (*m/z* 231); SEK4 and SEK4b (*m/z* 317). (*B*) Culture supernatants of *E. coli* strains expressing AaOKS, AaPKS4 and AaPKS5 when different concentrations of cerulenin was added to the medium. (*C*) Optical density (absorbance) of culture supernatants of *E. coli* strains expressing AaOKS, AaPKS4 and AaPKS5 at different wavelengths. CT, control (*E. coli* BL21(DE3) harboring pET-30a(+)). The data points represent the average values of three biological replicates.

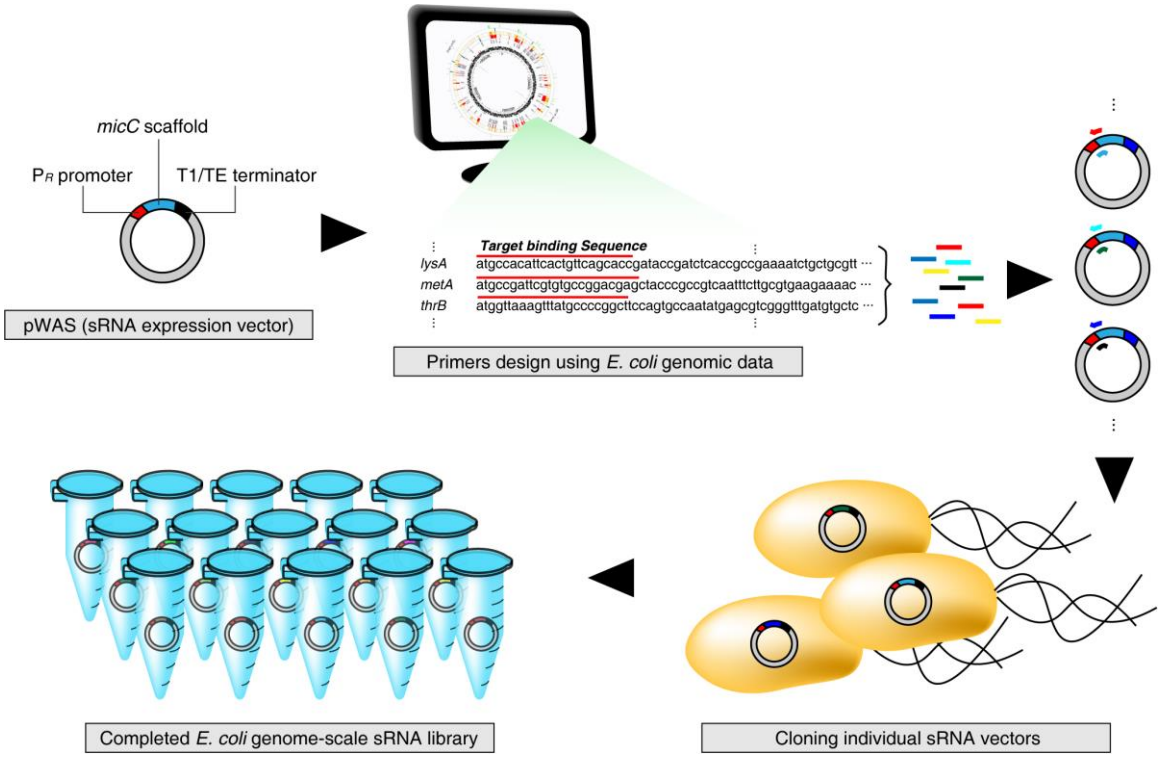

Fig. S4. Schematic procedures of the *E. coli* genome-scale synthetic sRNA library construction. For the sRNA expression vector, the pWAS vector harboring P_R promoter, *micC* scaffold and T1/TE terminator was utilized. Using the primers designed from the *E. coli* genomic data, site-directed mutagenesis was performed to insert target binding sequences, employing inverse PCR reactions followed by blunt-end ligation. Correct clones were identified and stored as the library components, both as plasmids and as strains harboring the plasmids.

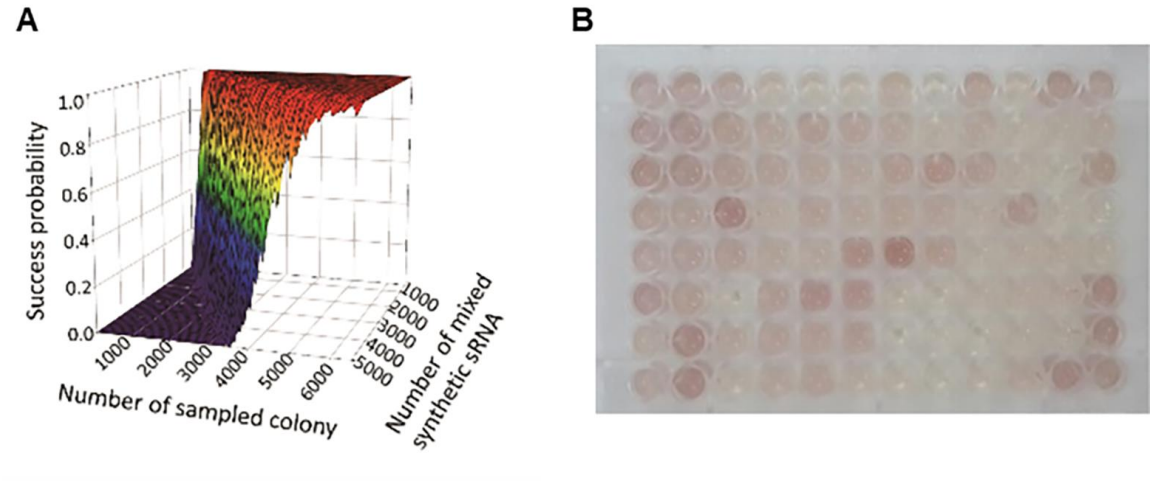

Fig. S5. High-throughput screening of *E. coli* genome-scale synthetic sRNA library using the RppA biosensor. (*A*) Averaged success probabilities. The minimum number of colonies (cells) that should be sampled with respect to the number of mixed synthetic sRNAs. The minimum numbers of cells to sample were calculated based on the Monte Carlo method (36). The result represents that 6-fold larger sample number when compared to the number of mixed synthetic sRNAs is sufficient to cover the whole library. Success probability (z axis) denotes the coverage of sampled synthetic sRNAs over the total number of mixed synthetic sRNAs. For this Monte Carlo simulation, we assumed that one single cell contains only one type of synthetic sRNA and the occurrence probability of respective synthetic sRNAs is the same. For each case, we randomly select a cell (corresponding to one synthetic sRNA) and this random selection was iterated according to the number of tested samples. The success probability is then calculated. We repeated this process 1,000 times and calculated an averaged success probability. (*B*) A representative view of a 96-well microplate used for high-throughput screening. Each well contains the culture of RppA expressing *E. coli* strain introduced with the genome-scale synthetic sRNA library components.

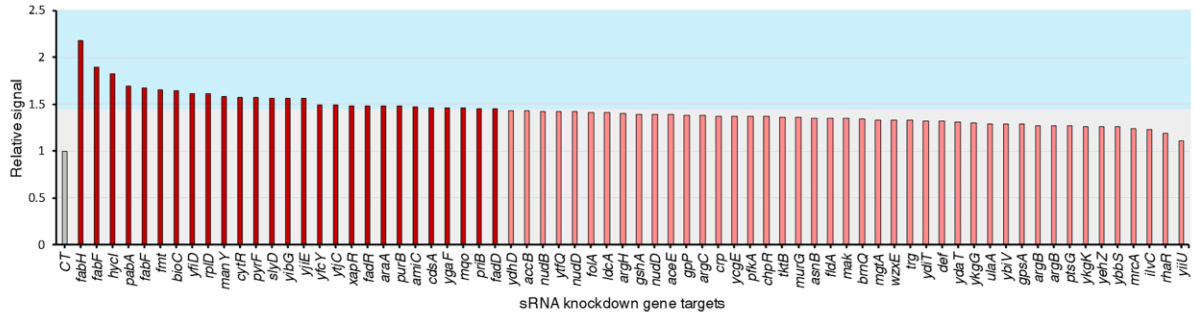

Fig. S6. Initial high-throughput screening results with regard to sRNA knockdown gene targets for enhanced intracellular malonyl-CoA accumulation using the RppA biosensor. The graph is divided into two sections – blue and grey – according to the set threshold (45% increase in signal when compared to the control *E. coli* BL21(DE3) strain). The 26 genes noted as deeper red bars denote the selected knockdown gene targets for further experiments.

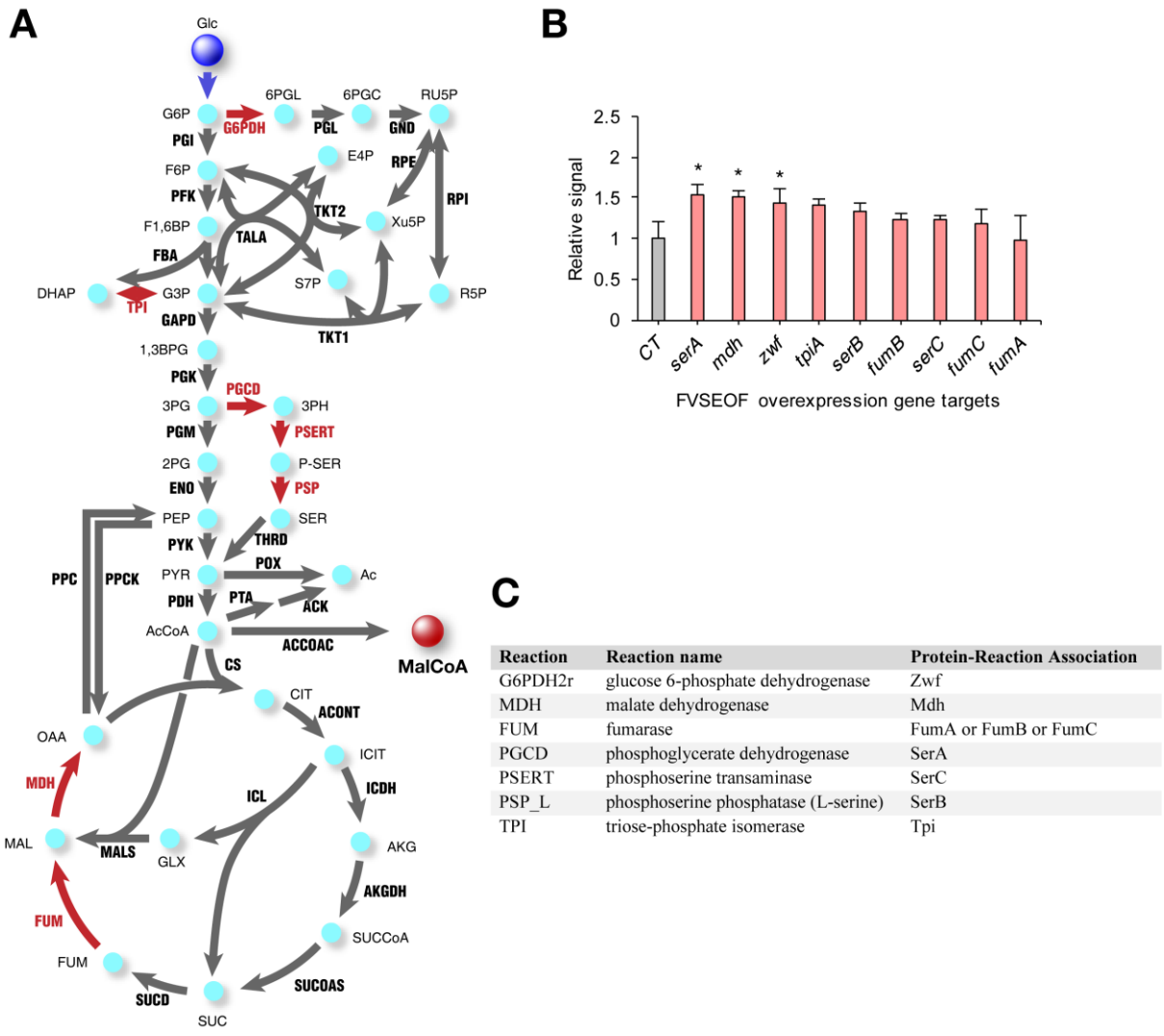

C

Reaction	Reaction name	Protein-Reaction Association
G6PDH2r	glucose 6-phosphate dehydrogenase	Zwf
MDH	malate dehydrogenase	Mdh
FUM	fumarase	FumA or FumB or FumC
PGCD	phosphoglycerate dehydrogenase	SerA
PSERT	phosphoserine transaminase	SerC
PSP_L	phosphoserine phosphatase (L-serine)	SerB
TPI	triose-phosphate isomerase	Tpi

Fig. S7. FVSEOF *in silico* simulation to identify overexpression gene targets for increased malonyl-CoA accumulation. (*A*) The biosynthetic pathway from glucose to malonyl-CoA. Letters in bold denote reactions, and plain letters denote metabolites except for MalCoA (malonyl-CoA). Grey arrows denote metabolic fluxes, and red arrows denote metabolic fluxes identified as overexpression targets by the FVSEOF *in silico* analysis. (*B*) Relative signals from sensor strains overexpressed with the FVSEOF target genes (*Text S3*). All error bars, mean ± SD ($n = 3$). *$P < 0.05$, determined by two-tailed Student's *t*-test. (*C*) The simulation results and the overexpression target genes identified by the FVSEOF algorithm. Abbreviations for the metabolites are: Glc, glucose; G6P, glucose 6-phosphate; F6P, fructose 6-phosphate; F1,6BP, fructose 1,6-bisphosphate; DHAP, dihydroxyacetone phosphate; G3P, glyceraldehyde-3-

phosphate; 1,3BPG, 1,3-bisphosphoglycerate; 3PG, 3-phosphoglycerate; 2PG, 2-phosphoglycerate; PEP, phosphoenolpyruvate; PYR, pyruvate; AcCoA, acetyl-CoA; Ac, acetate; 6PGL, 6-phosphoglucono-1,5-lactone; 6PGC, 6-phosphogluconate; Ru5P, ribulose-5-phosphate; E4P, D-erythrose-4-phosphate; Xu5P, xylulose 5-phosphate; S7P, sedoheptulose 7-phosphate; R5P, ribose 5-phosphate; 3PH, 3-phosphonooxypyruvate; P-SER, phosphoserine; SER, L-serine; CIT, citrate; ICIT, isocitrate; AKG, α-ketoglutarate; SUCCoA, succinyl-CoA; SUC, succinate; FUM, fumarate; MAL, malate; OAA, oxaloacetate. Abbreviations for the reactions are: PGI, glucose 6-phosphate isomerase; PFK, 6-phosphofructokinase; FBA, fructose-bisphosphate aldolase; TPI, triose-phosphate isomerase; GAPD, glyceraldehyde 3-phosphate dehydrogenase; PGK, phosphoglycerate kinase; PGM, phosphoglucomutase; ENO, enolase; PYK, pyruvate kinase; PDH, pyruvate dehydrogenase; PPC, phosphoenolpyruvate carboxylase; PPCK, phophoenolpyruvate carboxykinase; G6PDH, glucose 6-phosphate dehydrogenase; PGL, 6-phosphogluconolactonase; GND, 6-phosphogluconate dehydrogenase; RPE, ribulose-phosphate 3-epimerase; RPI, ribose 5-phosphate isomerase; TALA, transaldolase; TKT1, transketolase 1; TKT2, transketolase 2; PGCD, phosphoglycerate dehydrogenase; PSERT, phosphoserine transaminase; PSP, phosphoserine phosphatase; THRD, threonine dehydratase; POX, pyruvate dehydrogenase; PTA, phosphate acetyltransferase; ACK, acetate kinase; ACCOAC, acetyl-CoA carboxylase; CS, citrate synthase; ACONT, aconitase; ICDH, isocitrate dehydrogenase; AKGDH, α-ketoglutarate dehydrogenase; SUCCOAS, succinyl-CoA synthetase; SUCD, succinate dehydrognease; FUM, fumarase; MDH, malate dehydrogenase.

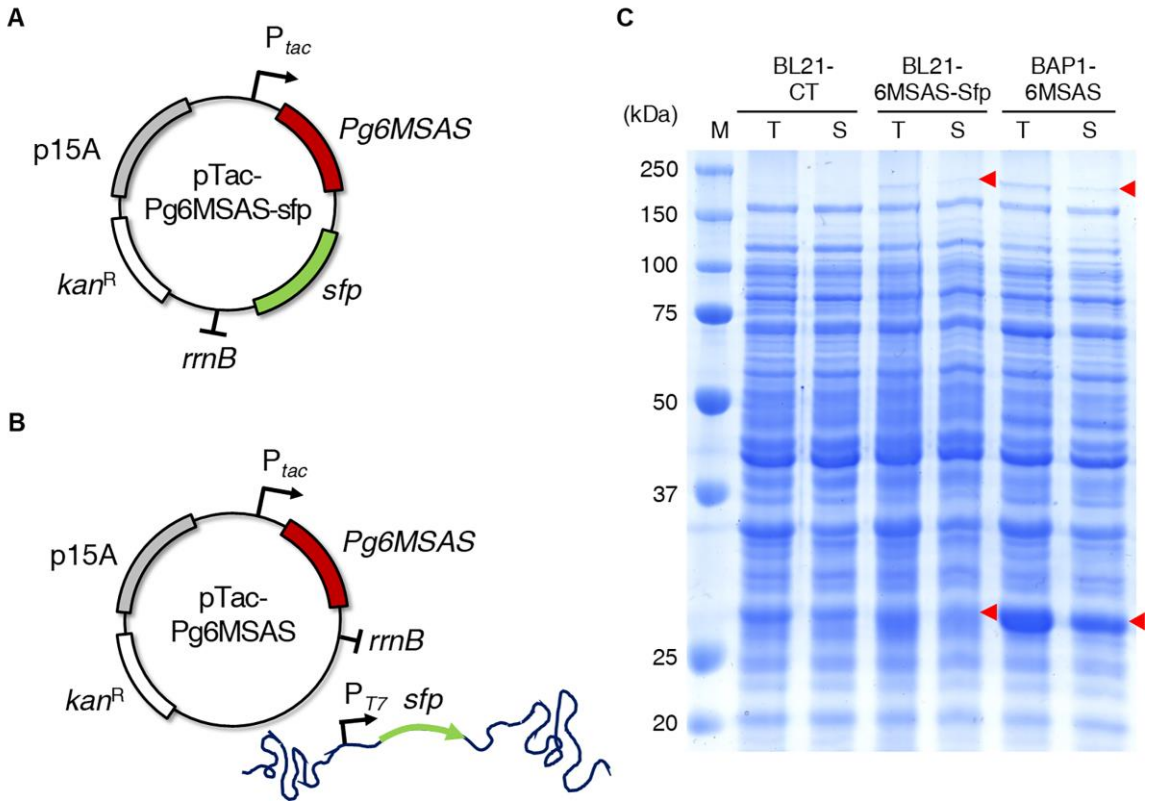

Fig. S8. Different genetic constructs for the expression of Pg6MSAS and Sfp. (*A*) Plasmid configuration of pTac-Pg6MSAS-sfp. (*B*) Plasmid configuration of pTac-Pg6MSAS and depiction of the *sfp* gene integrated into the chromosome of *E. coli* BL21(DE3) (*E. coli* BAP1 strain). (*C*) SDS-PAGE analysis for Pg6MSAS and Sfp expression. The upper red arrows denote *P. griseofulvum* 6MSAS (188 kDa). The lower red arrows denote *B. subtilis* Sfp (26.1 kDa). BL21-CT corresponds to the control strain of *E. coli* BL21(DE3) harboring pTac15K. Both Pg6MSAS and Sfp expression were enhanced in the *E. coli* BAP1 strain (*Text S4*). M, protein size marker; T, total fraction; S, soluble fraction.

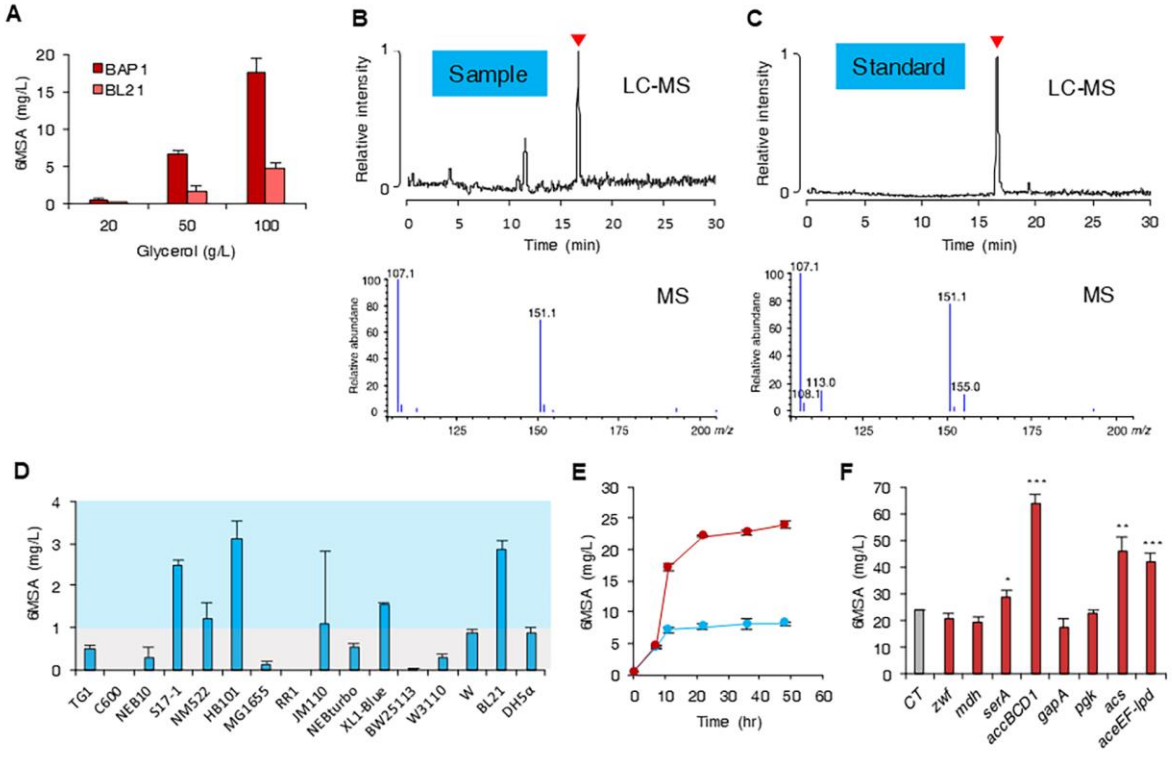

Fig. S9. Biosynthesis of 6MSA in engineered *E. coli* strains. (*A*) The highest 6MSA production can be achieved at 100 g/L of glycerol supplementation for both *E. coli* BL21(DE3) and BAP1 based strains. (*B*) LC-MS chromatogram (R_t 16.6 min) and MS spectrum (*m/z* 151.1 $[M\text{-}H]^-$, *m/z* 107.1 $[M\text{-}CO_2]^-$) of 6MSA produced from an engineered *E. coli*. (*C*) LC-MS chromatogram and MS spectrum of authentic 6MSA standard. The molecular weight of 6MSA is 152.147 g/mol. In (*C*) and (*D*), the red arrows denote the LC-MS 6MSA peaks corresponding to the MS spectra below. (*D*) Test tube scale cultivation of the given 16 *E. coli* strains introduced with the 6MSA biosynthetic pathway. The graph is divided into two sections – blue and grey – according to the set threshold (1 mg/L of 6MSA production) for selecting the strains for further experiments. (*E*) Time-course 6MSA production from *E. coli* BL21(DE3) harboring pTac-Pg6MSAS-sfp and pWAS-anti-pabA (blue line) and *E. coli* BAP1 harboring pTac-Pg6MSAS and pWAS-anti-pabA (red line). (*F*) Production of 6MSA from shake flask cultivation of *E. coli* BAP1 harboring pTac-Pg6MSAS and pWAS-anti-pabA (denoted as CT) additionally

overexpressed with the given genes. All error bars, mean ± SD (n = 3). *P < 0.05, **P < 0.01, ***P < 0.001, determined by two-tailed Student's t-test.

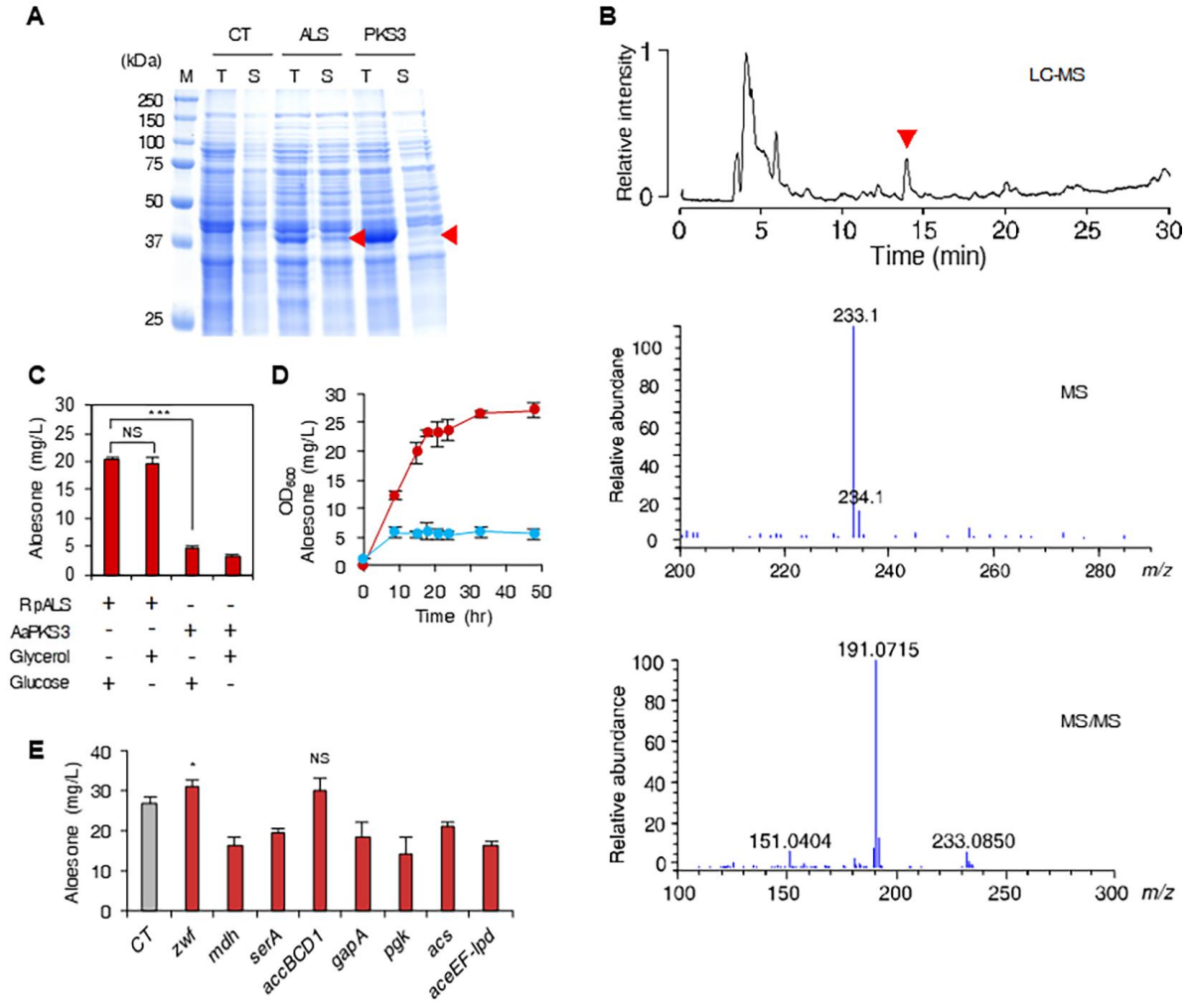

Fig. S10. Biosynthesis of aloesone in engineered *E. coli* strains. (*A*) SDS-PAGE analysis for RpALS and AaPKS3 expression. The red arrows denote RpALS (43 kDa) and AaPKS3 (44 kDa), respectively. CT corresponds to the control strain *E. coli* BL21(DE3) harboring pCDFDuet-1. M, protein size marker; T, total fraction; S, soluble fraction. (*B*) LC-MS chromatogram (R_t 13.9 min), MS spectrum (*m/z* 233.1 $[M+H]^+$) and MS/MS fragmentation pattern of aloesone (*m/z* 233.0850 $[M+H]^+$, *m/z* 191.0715 $[M+H-(CH_2CO)]^+$, *m/z* 151.0404 $[M+H-(CH3–CO–CH2–C=CH)]^+$) extracted from the culture of *E. coli* BL21(DE3) harboring pCDF-RpALS. The molecular weight of aloesone is 232.235 g/mol. The red arrow denotes the LC-MS aloesone peak corresponding to the MS spectrum below. (*C*) Aloesone production in engineered *E. coli* strains. The +/– signs for RpALS/AaPKS3 mean that RpALS/AaPKS3 was

expressed/not expressed in *E. coli* BL21(DE3). The +/– signs for glycerol/glucose mean that glycerol/glucose was used/unused as carbon sources. (*D*) Time-course shake flask cultivation of *E. coli* BL21(DE3) harboring pCDF-RpALS and pWAS-anti-pabA. The red line denotes aloesone production and the blue line denotes cell growth represented as OD_{600}. (*E*) Production of aloesone from shake flask cultivation of *E. coli* BL21(DE3) harboring pCDF-RpALS and pWAS-anti-pabA (denoted as CT) additionally overexpressed with the given genes. Error bars, mean ± SD (n = 3). NS, not significant; *P < 0.05, ***P < 0.001; determined by two-tailed Student's t-test.

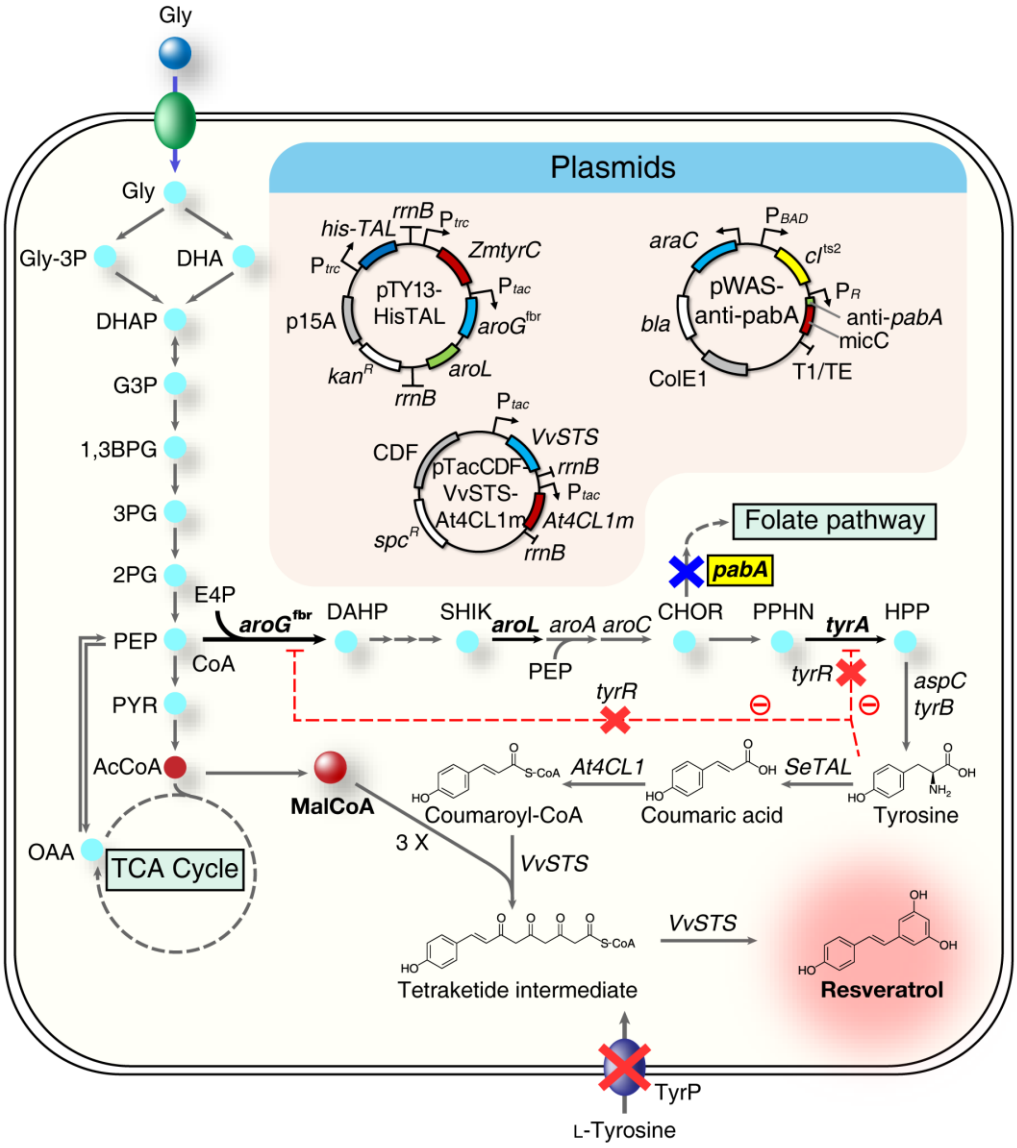

Fig. S11. The resveratrol biosynthetic pathway from glycerol. Red X indicates that the corresponding gene cluster was knocked out. Blue X (along with gene written in bold letters surrounded by yellow box) indicates that the corresponding gene was knocked down. Grey dotted lines indicate omitted pathways. Thick black arrows along with genes written in bold letters denote overexpressed metabolic fluxes. Red dotted lines (along with – signs in circles) indicate transcriptional repression. Black dotted lines (along with + signs in circles) indicate transcriptional activation. The upper box describes the introduced plasmids. Abbreviations: Gly, glycerol; Gly-3P, glycerol 3-phosphate; DHA, dihydroxyacetone; DHAP,

dihydroxyacetone phosphate; G3P, glyceraldehyde 3-phosphate; 1,3BPG, 1,3-bisphosphoglycerate; 3PG, 3-phosphoglycerate; 2PG, 2-phosphoglycerate; PEP, phosphoenolpyruvate; PYR, pyruvate; OAA, oxaloacetate; E4P, D-erythrose 4-phosphate; DAHP, 3-deoxy-D-arabinoheptulosonate 7-phosphate; SHIK, shikimate; CHOR, chorismate; PPHN, prephenate; HPP, 4-hydroxyphenylpyruvate; FOR, formate; AcCoA, acetyl-CoA; MalCoA, malonyl-CoA. *bla*, beta-lactamase gene; kan^R, kanamycin-resistance gene; spc^R, spectinomycin-resistance gene; p15A, replication origin; ColE1, replication origin; CDF, replication origin; P_{tac}, *tac* promoter; P_{BAD}, arabinose-inducible promoter; P_R, P_R promoter; P_{trc}, *trc* promoter; *rrnB*, *rrnBT1T2* terminator; T1/TE, terminator.

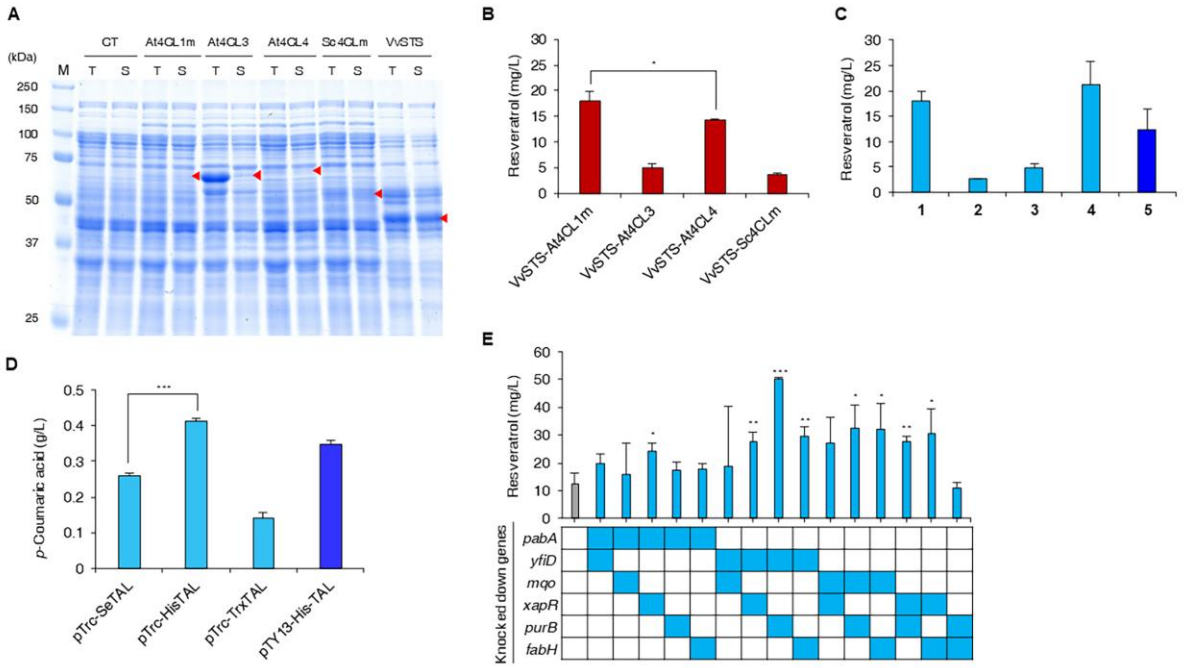

Fig. S12. Biosynthesis of resveratrol in engineered *E. coli* strains. (*A*) SDS-PAGE analysis for At4CL1m (61.1 kDa), At4CL3 (61.3 kDa), At4CL4 (62.6 kDa), Sc4CLm (55.3 kDa) and VvSTS (42.8 kDa) expression. The red arrows denote the corresponding enzymes. CT corresponds to the control strain *E. coli* BL21(DE3) harboring pTac15K. M, protein size marker; T, total fraction; S, soluble fraction. (*B*) Resveratrol production from *p*-coumaric acid by expressing the combinations of VvSTS and different 4CLs. (*C*) Effects of different plasmid constructs on resveratrol production. The numbers on the x-axis denote strains harboring different plasmid constructs: 1, pTac-VvSTS-At4CL1m; 2, pTac-At4CL1m-opr-VvSTS (two genes in an operon); 3, pTac-At4CL1m-fus-VvSTS (for expression of a fusion protein of At4CL1m and VvSTS); 4 and 5, pTacCDF-VvSTS-At4CL1m. For the strains 1-4, the corresponding plasmids were introduced into *E. coli* BL21(DE3) and were cultivated in the presence of 2 mM *p*-coumaric acid and 20 g/L glycerol. For the strain 5, the corresponding plasmid was introduced into the *p*-coumaric acid producer BTY5 harboring pTY13-HisTAL, and 20 g/L of glycerol was used as the sole carbon source. Strain 5 (the base strain for resveratrol production) is noted as the deeper blue bar. (*D*) Production of *p*-coumaric acid by

attaching different N-terminal tags to SeTAL. Except for pTY13-HisTAL, each of the corresponding vectors was introduced into the BTY5.13, the L-tyrosine producer. Production of *p*-coumaric acid from BTY5 harboring the plasmid pTY13-HisTAL is represented as the deeper blue bar. (*E*) Combinatorial double knockdown of the six selected gene targets from Fig. 5*A* for resveratrol production. Control (without sRNA) is noted as the grey bar. The genes corresponding to the filled squares under each bar denote knocked down genes. All error bars, mean ± SD ($n = 3$). *$P < 0.05$, **$P < 0.01$, ***$P < 0.001$, determined by two-tailed Student's *t*-test.

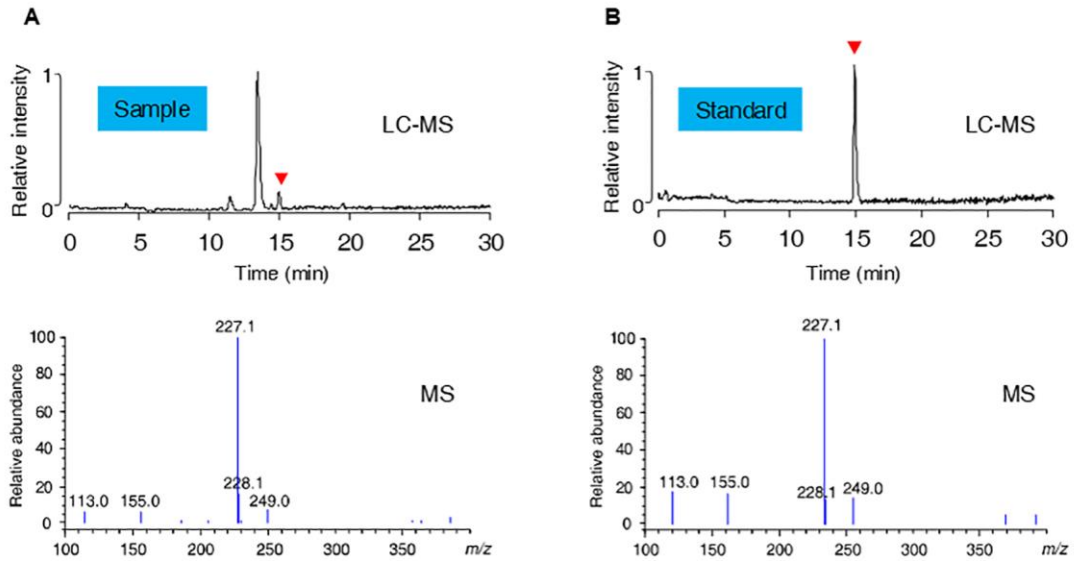

Fig. S13. LC-MS analysis of the culture sample and authentic standard of resveratrol. (*A*) LC-MS chromatogram (R_t 13.4 min) and MS spectrum (*m/z* 227.1 $[M-H]^-$) of resveratrol produced from an engineered *E. coli*. (*B*) LC-MS chromatogram and MS spectrum of the authentic resveratrol standard. The molecular weight of resveratrol is 228.247 g/mol.

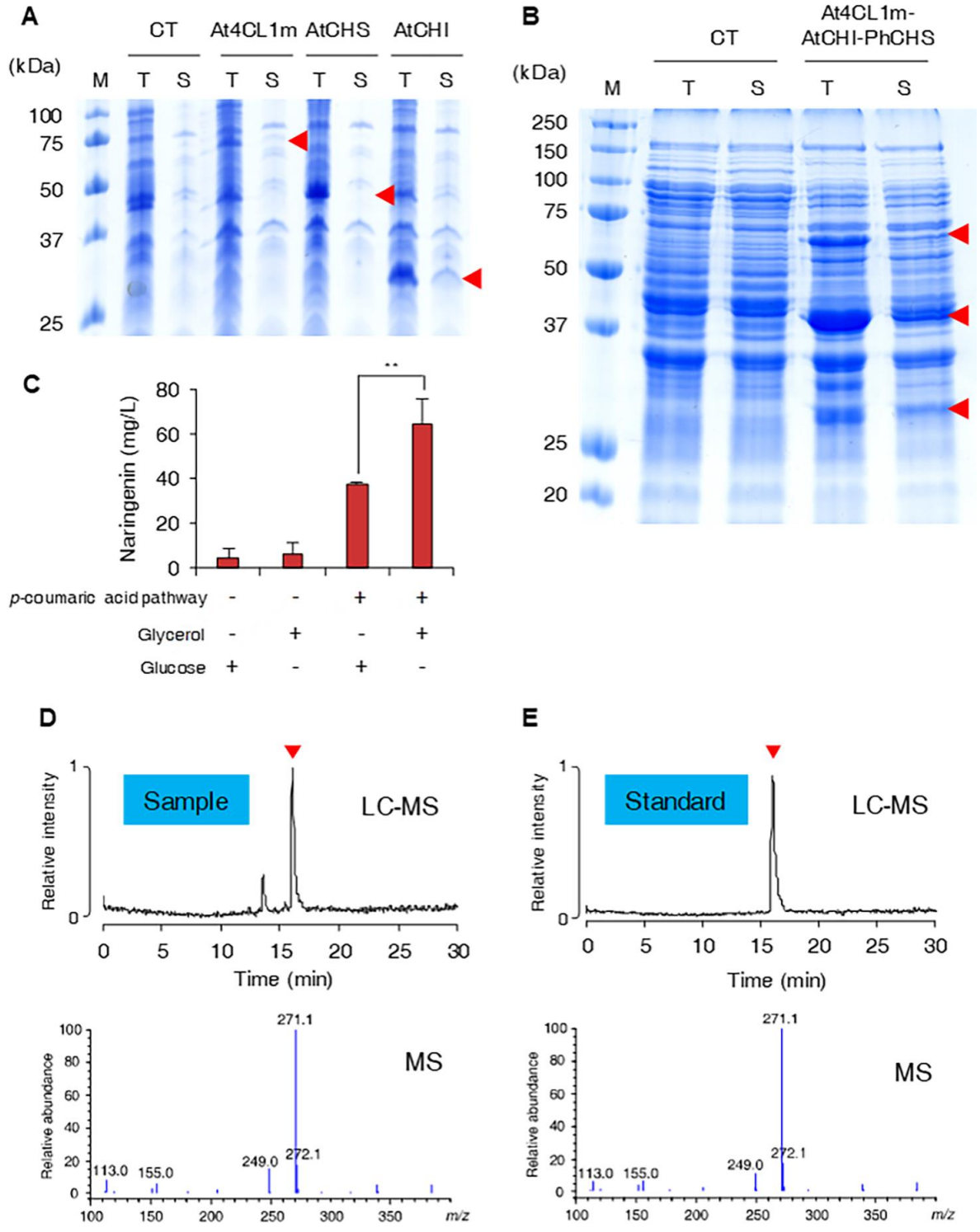

Fig. S14. Biosynthesis of naringenin in engineered *E. coli* strains. (*A*) SDS-PAGE analysis for the expression of At4CL1m (61.1 kDa), AtCHS (43.1 kDa) and AtCHI (26.6 kDa). The red arrows denote the corresponding enzymes. (*B*) SDS-PAGE analysis for the expression of At4CL1m, PhCHS (42.6 kDa) and AtCHI. The red arrows denote, from the top, A4CL1m,

PhCHS and AtCHI. In (*A*) and (*B*), CT corresponds to the control strain *E. coli* BL21(DE3) harboring pCDFDuet-1; M, protein size marker; T, total fraction; S, soluble fraction. (*C*) Naringenin production from the strains harboring pTrcCDF-At4CL1m-AtCHI-PhCHS. For the strains harboring *p*-coumaric acid pathway, the pTrcCDF-At4CL1m-AtCHI-PhCHS plasmid was introduced into the *p*-coumaric acid producer (BTY5 harboring pTY13-HisTAL). For the strains without *p*-coumaric acid pathway, the plasmid was introduced into *E. coli* BL21(DE3) and 2 mM of *p*-coumaric acid was exogenously fed. Either 20 g/L of glucose or glycerol was supplemented to the medium. Error bars, mean ± SD (n = 3). (*D*) LC-MS chromatogram (R_t 16.0 min) and MS spectrum (*m/z* 271.1 $[M-H]^-$) of naringenin produced from an engineered *E. coli*. (*E*) LC-MS chromatogram and MS spectrum of authentic naringenin standard. The molecular weight of naringenin is 272.256 g/mol. $^{**}P < 0.01$, determined by two-tailed Student's *t*-test.

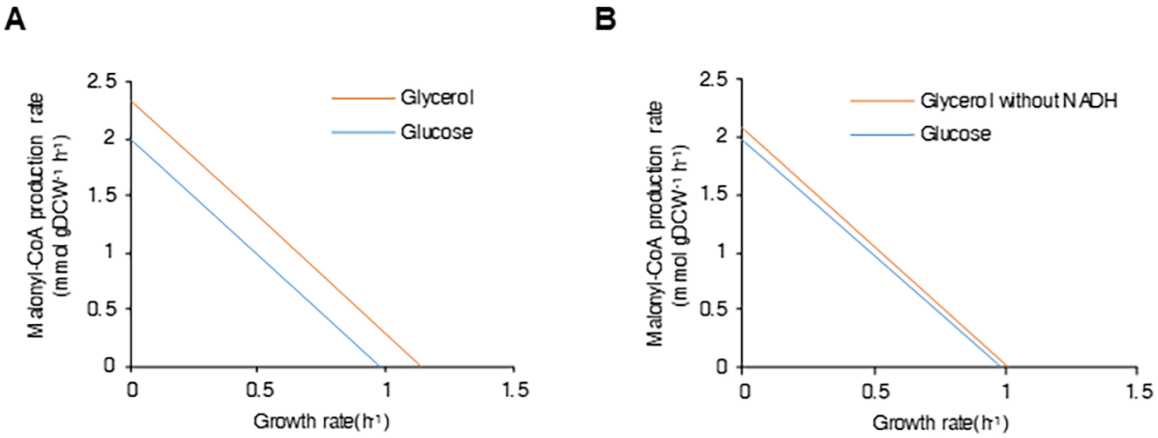

Fig. S15. Effect of different carbon sources on malonyl-CoA flux. (*A*) Malonyl-CoA production rate according to varying growth rate of *E. coli* when either glycerol or glucose was supplemented as a sole carbon source, respectively. Flux response analysis was employed. (*B*) Malonyl-CoA production rate according to varying growth rate of *E. coli* when either glycerol or glucose was supplemented as a sole carbon source, respectively. Here, the beneficial effect of NADH regeneration by using glycerol was excluded from consideration. Flux response analysis was employed.

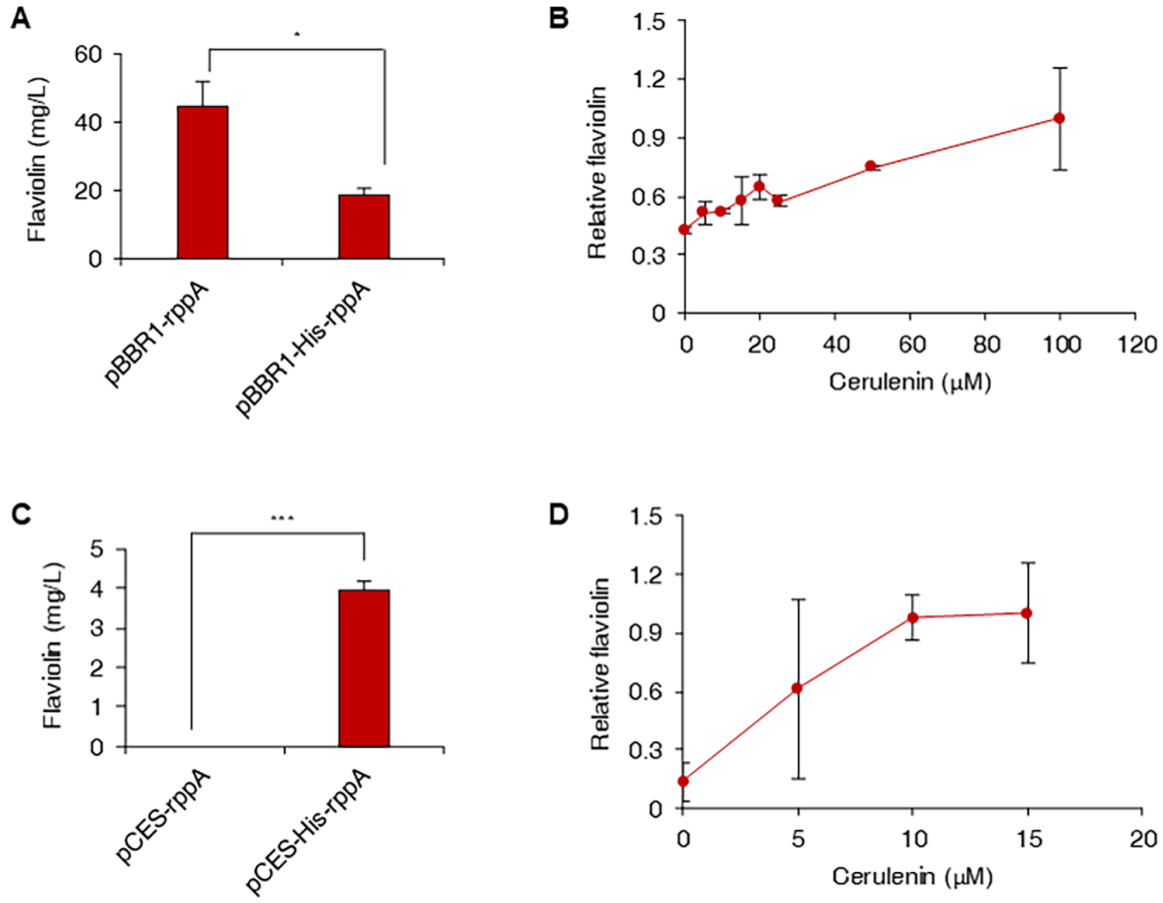

Fig. S16. RppA is also functional in *P. putida* and *C. glutamicum*. (*A*) Flaviolin production from *P. putida* harboring pBBR1-rppA or pBBR1-His-rppA. (*B*) Relative flaviolin production from *P. putida* harboring pBBR1-rppA normalized with cell growth increases with increased cerulenin concentration. Flaviolin concentration was measured by HPLC. (*C*) Flaviolin production from *C. glutamicum* harboring pCES-rppA or pCES-His-rppA. (*D*) Relative flaviolin production from *C. glutamicum* harboring pCES-His-rppA normalized with cell growth increases with increased cerulenin concentration. Flaviolin concentration was measured by HPLC. All error bars, mean ± SD (n = 3). *P < 0.05, ***P < 0.001, determined by two-tailed Student's t-test.

SI Appendix Tables

Table S1. Heterologous genes used in this study.

Gene	Organism	Accession Number *
Sgr_rppA	*Streptomyces griseus*	BAE07216
Sco_rppA	*Streptomyces coelicolor*	CAC01488
Sma_rppA	*Streptomyces avermitilis*	BAC74842
Sen_rppA	*Saccharopolyspora erythraea*	AAL78053
Sp_rppA	*Streptomyces peucetius*	ABY71276
Sac_rppA	*Streptomyces aculeolatus*	ABS50451
*whiE*_ORFII	*Streptomyces coelicolor*	CAB45605
AaPCS	*Aloe arborescens*	AAX35541
AaOKS	*Aloe arborescens*	AAT48709
AaPKS4	*Aloe arborescens*	ACR19997
AaPKS5	*Aloe arborescens*	ACR19998
sfp	*Bacillus subtilis*	ABV89950
Pg6MSAS	*Penicillium griseofulvum*	CAA39295
RpALS	*Rheum palmatum*	AAS87170
AaPKS3	*Aloe arborescens*	ABS72373
SeTAL	*Saccharothrix espanaensis*	CCH33126
At4CL1	*Arabidopsis thaliana*	AAQ86588
At4CL3	*Arabidopsis thaliana*	AAQ86589
At4CL4	*Arabidopsis thaliana*	Q9LU36
Sc4CL	*Streptomyces coelicolor*	CAB95894
PhCHS	*Petunia x hybrida*	AGZ04577
AtCHI	*Arabidopsis thaliana*	NP_191072
VvSTS†	*Vitis vinifera*	CAA54221

* Denote NCBI accession numbers for the enzyme sequences.

† The corresponding gene was codon optimized for *E. coli* K-12 MG1655.

Table S2. The list of *E. coli* strains used in this study.

Strains	Description	Source
DH5α	F^{-} φ80 *lacZΔM15 Δ(lacZYA-argF)*U169 *recA1 endA1* hsdR17 *(r_K^-, m_K^+) phoA supE44 thi-1 gyrA96 relA1* λ$^-$	Invitrogen
TG1	F' *[traD36 proAB$^+$ lacI^q lacZΔacZZsupE thi-1 i-1 Z proAB) oAmcrB-hsdSM)5, (r_K^- m_K^-)*	Lucigen Corporation
C600	F$^-$ *supE44 tonA21 thi-1 thr-1 leuB6 lacY1* λ$^-$	(37)
NEB10	*araD139* Δ*(ara-leu)7697 fhuA lacX74 galK (*φ80 Δ*(lacZ)M15) mcrA galU recA1 endA1 nupG rpsL (Str^r)* Δ*(mrr-hsdRMS-mcrBC)*	New England BioLabs
S17-1	Mobilizing donor strain, *pro recA*, which has an RP4 derivative integrated into the chromosome	(38)
NM522	F' *proA$^+$B$^+$ lacI^q Δ(lacZ)M15/ Δ(lac-proAB) glnV thi-1 Δ(hsdS-mcrB)5*	New England BioLabs
HB101	F$^-$ *Δ(gpt-proA)62 leuB6 glnV44 ara-14 galK2 lacY1 Δ(mcrC-mrr) rpsL20 (Str^r) xyl-5 mtl-1 recA13*	(39)
MG1655	F$^-$ λ$^-$ *ilvG- rfb-50 rph-1*	(40
RR1	F$^-$ *supE44 lacY1 ara-14 galK2 xyl-5 mtl-1 leuB6 proA2 Δ(mcrC-mrr) recA$^+$ rpsL20 thi-1* λ$^-$	(41)
JM110	*rpsL (Str^r) thr leu thi-1 lacY galK galT ara tonA tsx dam dcm supE44 Δ(lac-proAB) [F´ traD36 proAB lacIqZΔM15]*	Stratagene
NEBturbo	F' *proA$^+$B$^+$ lacIq* Δ*lacZM15/ fhuA2* Δ*(lac-proAB) glnV gal R(zgb-210::Tn10)Tets endA1 thi-1* Δ*(hsdS-mcrB)5*	New England BioLabs
XL1-Blue	*recA1 endA1 gyrA96 thi-1 hsdR17 supE44 relA1 lac* [F´ *proAB lacIqZΔM15 Tn10 (Tet^r)*]	Stratagene
BW25113	F$^-$ Δ*(araD-araB)567 lacZ4787::rrnB-3 rph-1 Δ(rhaD-rhaB)568 hsdR514* λ$^-$	Coli Genetics Stock Center
W3110	K12 F$^-$ *(rmD-rmE)*	(42)
W3110(DE3)	W3110 (DE3)	(42)
W	ATCC 9637	(43)
BL21(DE3)	F$^-$ *ompT hsdSB (rB-mB-) gal dcm* (DE3)	Invitrogen
BAP1	BL21 (DE3) Δ*prpRBCD::*P*T7-sfp*-P*T7-prpE*	(12)
BTY5	BL21 (DE3) Δ*tyrR* Δ*tyrP*	(31)
BTY5.13	BTY5 harboring pTY13	(31)

Table S3. The list of 14 sRNA knockdown gene targets and their characteristics.

No.	Target gene	Protein function	Essentiality‡
1	*fabH*	3-oxoacyl-[acyl-carrier-protein] synthase III	NE
2	*fabF*	3-oxoacyl-[acyl-carrier-protein] synthase II	NE
3	*cytR*	LacI family transcriptional regulator, repressor for *deo* operon, *udp*, *cdd*, *tsx*, *nupC* and *nupG*	NE
4	*yfcY*	beta-ketoacyl-CoA thiolase	NE
5	*fmt*	10-formyltetrahydrofolate:L-methionyl-tRNA(fMet)N-formyltransferase	ND
6	*mqo*	malate dehydrogenase, FAD/NAD(P)-binding domain	ND
7	*fadR*	GntR family transcriptional regulator, negative regulator for fad regulon and positive regulator of *fabA*	NE
8	*yfiD*	pyruvate formate lyase subunit	NE
9	*purB*	adenylosuccinate lyase	NE
10	*xapR*	transcriptional activator of *xapAB*	NE
11	*araA*	L-arabinose isomerase	ND
12	*pyrF*	orotidine-5'-phosphate decarboxylase	E
13	*pabA*	aminodeoxychorismate synthase, subunit II	E
14	*hycI*	protease involved in processing C-terminal end of HycE	NE

‡ E, essential; NE, non-essential; ND, not determined; essentiality was determined upon the growth of *E. coli* in minimal medium supplemented with simple carbon sources when the corresponding gene was knocked out, as is reported in the metacyc database (44).

Table S4. The list of plasmids used in this study.

Plasmids	**Description**[§]	**Source**	**Accession number**[¶]
pET-30a(+)	Km^R, *T7* promoter, ColE1 origin, *lac*I^q, 5.4-kb	Novagen	
pET-Sgr_rppA	pET-30a(+) derivative containing *Sgr_rppA* from *S. griseus*	This study	MH473344
pET-Sco_rppA	pET-30a(+) derivative containing *Sco_rppA* from *S. coelicolor*	This study	MH488902
pET-Sma_rppA	pET-30a(+) derivative containing *Sma_rppA* from *S. avermitilis*	This study	MH488903
pET-Sen_rppA	pET-30a(+) derivative containing *Sen_rppA* from *S. erythraea*	This study	MH488904
pET-Sp_rppA	pET-30a(+) derivative containing *Sp_rppA* from *S. peucetius*	This study	MH488905
pET-Sac_rppA	pET-30a(+) derivative containing *Sac_rppA* from *S. aculeolatus*	Lab stock	MH488906
pET-Sgr_rppA_whiE	pET-30a(+) derivative containing *Sgr_rppA* from *S. griseus* and *whiE*_ORFII from *S. coelicolor*	This study	MH488907
pCDFDuet-1	Spc^R, *T7* promoter, CDF origin, *lac*I^q, 3.8-kb	Novagen	
pTac15K	Km^R, *tac* promoter, p15A origin, 4.0-kb	(3)	MH488908
pTrc99A	Ap^R, *trc* promoter, pBR322 (ColE1) origin, *lac*I^q, 4.2-kb	(3)	U13872.1
pTacCDFS	pCDFDuet-1 derivative with the *T7* based expression cassette was exchanged with P*tac* – MCS – *rrnBT1T2*$_T$ from pTac15K	This study	MH488909
pTrcCDFS	pCDFDuet-1 derivative with the *T7* based expression cassette was exchanged with P*trc* – MCS – *rrnBT1T2*$_T$ from pTrc99A	This study	MH488910
pTac-Sgr_rppA	pTacCDFS derivative containing *Sgr_rppA*	This study	MH488911
pTac-5'UTR-Sgr_rppA	pTacCDFS derivative containing 5'-UTR modified *Sgr_rppA*	This study	MH473345
pET-AaPCSm	pET-30a(+) derivative containing mutated *PCS* from *A. arborescens* (AaPCSm; M207G)	This study	MH651713
pET-AaOKS	pET-30a(+) derivative containing *OKS* from *A. arborescens*	This study	MH651714
pET-AaPKS3m	pET-30a(+) derivative containing mutated *PKS3* from *A. arborescens* (AaPKS3m; A207G)	This study	MH651715
pET-AaPKS4	pET-30a(+) derivative containing *PKS4* from *A. arborescens*	This study	MH651716
pET-AaPKS5	pET-30a(+) derivative containing *PKS5* from *A. arborescens*	This study	MH651717
pBBR1MCS-2	Km^R, pBBR1 origin, 5.1-kb.	(45)	U23751.1

Plasmids	Description[§]	Source	Accession number[¶]
pTac-His-Sgr_rppA	pTacCDFS derivative containing *rppA* from *S. griseus* with N-terminal poly-His-tag.	This study	MH488951
pBBR1-rppA	pBBR1MCS-2 derivative containing *rppA* from *S. griseus.*	This study	MH488952
pBBR1-His-rppA	pBBR1MCS-2 derivative containing *rppA* from *S. griseus* with N-terminal poly-His-tag.	This study	MH488953
pCES-H36-GFP	Km^R, pCES208 derivative, containing eGFP under P_{H36}, 6.7 kb.	(46)	
pCES-rppA	pCES208 derivative containing *rppA* from *S. griseus*.	This study	
pCES-His-rppA	pCES208 derivative containing *rppA* from *S. griseus* with N-terminal poly-His-tag.	This study	
pWAS	Ap^R, ColE1 origin, synthetic sRNA expression vector containing *araC*, cI^{ts2} and synthetic sRNA expression cassette (P_R promoter – *micC* – $T1TE_T$), 4.9-kb	(6)	MH488912
pTrc-zwf	pTrc99A derivative containing *zwf* from *E. coli* BL21(DE3)	This study	MH488913
pTrc-mdh	pTrc99A derivative containing *mdh* from *E. coli* BL21(DE3)	This study	MH488914
pTrc-fumA	pTrc99A derivative containing *fumA* from *E. coli* BL21(DE3)	This study	MH488915
pTrc-fumB	pTrc99A derivative containing *fumB* from *E. coli* BL21(DE3)	This study	MH488916
pTrc-fumC	pTrc99A derivative containing *fumC* from *E. coli* BL21(DE3)	This study	MH488917
pTrc-serA	pTrc99A derivative containing *serA* from *E. coli* BL21(DE3)	This study	MH488918
pTrc-serB	pTrc99A derivative containing *serB* from *E. coli* BL21(DE3)	This study	MH488919
pTrc-serC	pTrc99A derivative containing *serC* from *E. coli* BL21(DE3)	This study	MH488920
pTrc-tpiA	pTrc99A derivative containing *tpiA* from *E. coli* BL21(DE3)	This study	MH488921
pTac-Pg6MSAS	pTac15K derivative containing *6MSAS* from *P. griseofulvum*	This study	MH488922
pTac-Pg6MSAS-sfp	pTac15K derivative containing *6MSAS* from *P. griseofulvum* and *sfp* from *B. subtilis*	This study	MH488924
pTac15K-sfp	pTac15K derivative containing *sfp* from *B. subtilis*	This study	MH488923
pCDF-RpALS	pCDFDuet-1 derivative containing *ALS* from *R. palmatum*	This study	MH488925
pCDF-AaPKS3	pCDFDuet-1 derivative containing *PKS3* from *A. arborescens*	This study	MH488926
pBBR1MCS	Cm^R, pBBR1 origin, 4.7-kb.	(47)	U02374

Plasmids	Description[§]	Source	Accession number[¶]
pBBR1TaC	pBBR1MCS derivative harboring P*tac* – MCS – *rrnBT1T2*$_T$ from pTac15K	This study	MH651718
pBBR1-zwf	pBBR1TaC derivative containing *zwf* from *E. coli* BL21(DE3)	This study	MH651719
pBBR1-mdh	pBBR1TaC derivative containing *mdh* from *E. coli* BL21(DE3)	This study	MH651720
pBBR1-serA	pBBR1TaC derivative containing *serA* from *E. coli* BL21(DE3)	This study	MH651721
pBBR1-accBCD1	pBBR1TaC derivative containing *accBC* and *accD1* from *C. glutamicum* ATCC 13032	This study	MH651722
pBBR1-gapA	pBBR1TaC derivative containing *gapA* from *E. coli* BL21(DE3)	This study	MH651723
pBBR1-pgk	pBBR1TaC derivative containing *pgk* from *E. coli* BL21(DE3)	This study	MH651724
pBBR1-acs	pBBR1TaC derivative containing *acs* from *E. coli* BL21(DE3)	This study	MH651725
pBBR1-aceEF-lpd	pBBR1TaC derivative containing *aceEF* and *lpd* from *E. coli* BL21(DE3)	This study	MH651726
pTY13	pTac15K derivative containing *tyrC* from *Zymomonas mobilis* under P*trc* and *aroG*^{fbr} and *aroL* from *E. coli* K12 under P*tac*.	(31)	MH488927
pTrc-SeTAL	pTrc99A derivative containing *TAL* from *S. espanaensis*.	This study	MH488929
pTrc-HisTAL	pTrc99A derivative containing *TAL* from *S. espanaensis* with N-terminal poly-His-tag.	This study	MH488930
pTrc-TrxTAL	pTrc99A derivative containing *TAL* from *S. espanaensis* with *E. coli* thioredoxin N-terminal tag.	This study	MH488931
pTY13-HisTAL	pTY13 derivative additionally containing poly-His-tagged *SeTAL* under P*trc*.	This study	MH488928
pTac-At4CL1	pTac15K derivative containing *4CL1* from *A. thaliana.*	This study	MH488932
pTac-At4CL1m	pTac15K derivative containing mutated *4CL1* from *A. thaliana* (*At4CL1m*; I250L/N404K/I461V).	This study	MH488933
pTac-At4CL3	pTac15K derivative containing *4CL3* from *A. thaliana*.	This study	MH488934
pTac-At4CL4	pTac15K derivative containing *4CL4* from *A. thaliana*.	This study	MH488935
pTac-Sc4CL	pTac15K derivative containing *4CL* from *S. coelicolor*.	This study	MH488936
pTac-Sc4CLm	pTac15K derivative containing mutated *4CL* from *S. coelicolor* (*Sc4CLm*; A294G).	This study	MH488937
pTac-VvSTS	pTac15K derivative containing *STS* from *V. vinifera*.	This study	MH488938
pTac-VvSTS-At4CL1m	pTac15K derivative containing *VvSTS* under P*tac* and *At4CL1m* under P*tac*.	This study	MH488939
pTac-VvSTS-At4CL3	pTac15K derivative containing *VvSTS* under P*tac* and *At4CL3* under P*tac*.	This study	MH488940

Plasmids	Description[§]	Source	Accession number[¶]
pTac-VvSTS-At4CL4	pTac15K derivative containing *VvSTS* under P*tac* and *At4CL4* under P*tac*.	This study	MH488941
pTac-VvSTS-Sc4CLm	pTac15K derivative containing *VvSTS* under P*tac* and *Sc4CLm* under P*tac*.	This study	MH488942
pTac-At4CL1m-opr-VvSTS	pTac15K derivative containing *At4CL1m* and *VvSTS* under P*tac* as an operon.	This study	MH488943
pTac-At4CL1m-fus-VvSTS	pTac15K derivative for the expression of fusion protein At4CL1m – GGGS – VvSTS.	This study	MH488944
pTacCDF-VvSTS-At4CL1m	pTacCDFS derivative containing *VvSTS* under P*tac* and *At4CL1m* under P*tac*.	This study	MH488945
pTrc-At4CL1m-AtCHI-PhCHS	pTrc99A derivative containing *At4CL1m*, *CHI* from *A. thaliana* and *CHS* from *P. x hybrida.*	This study	MH488946
pTrcCDF-At4CL1m-AtCHI-PhCHS	pTrcCDFS derivative containing *At4CL1m*, *CHI* from *A. thaliana* and *CHS* from *P. x hybrida.*	This study	MH488947
pWAS-anti-fabH	pWAS derivative containing anti-*fabH* sRNA.	This study	
pWAS-anti-fabF	pWAS derivative containing anti-*fabF* sRNA.	This study	
pWAS-anti-cytR	pWAS derivative containing anti-*cytR* sRNA.	This study	
pWAS-anti-yfcY	pWAS derivative containing anti-*yfcY* sRNA.	This study	
pWAS-anti-fmt	pWAS derivative containing anti-*fmt* sRNA.	This study	
pWAS-anti-mqo	pWAS derivative containing anti-*mqo* sRNA.	This study	
pWAS-anti-fadR	pWAS derivative containing anti-*fadR* sRNA.	This study	
pWAS-anti-yfiD	pWAS derivative containing anti-*yfiD* sRNA.	This study	
pWAS-anti-purB	pWAS derivative containing anti-*purB* sRNA.	This study	
pWAS-anti-xapR	pWAS derivative containing anti-*xapR* sRNA.	This study	
pWAS-anti-araA	pWAS derivative containing anti-*araA* sRNA.	This study	
pWAS-anti-pyrF	pWAS derivative containing anti-*pyrF* sRNA.	This study	
pWAS-anti-pabA	pWAS derivative containing anti-*pabA* sRNA.	This study	MH488948
pWAS-anti-hycI	pWAS derivative containing anti-*hycI* sRNA.	This study	
pWAS-anti-pabA-anti-yfiD	pWAS derivative containing anti-*pabA* and anti-*yfiD* sRNA.	This study	
pWAS-anti-pabA-anti-mqo	pWAS derivative containing anti-*pabA* and anti-*mqo* sRNA.	This study	
pWAS-anti-pabA-anti-xapR	pWAS derivative containing anti-*pabA* and anti-*xapR* sRNA.	This study	
pWAS-anti-pabA-anti-purB	pWAS derivative containing anti-*pabA* and anti-*purB* sRNA.	This study	
pWAS-anti-pabA-anti-fabH	pWAS derivative containing anti-*pabA* and anti-*fabH* sRNA.	This study	
pWAS-anti-yfiD-anti-mqo	pWAS derivative containing anti-*yfiD* and anti-*mqo* sRNA.	This study	

Plasmids	Description[§]	Source	Accession number[¶]
pWAS-anti-yfiD-anti-xapR	pWAS derivative containing anti-*yfiD* and anti-*xapR* sRNA.	This study	
pWAS-anti-yfiD-anti-purB	pWAS derivative containing anti-*yfiD* and anti-*purB* sRNA.	This study	MH488949
pWAS-anti-yfiD-anti-fabH	pWAS derivative containing anti-*yfiD* and anti-*fabH* sRNA.	This study	
pWAS-anti-mqo-anti-xapR	pWAS derivative containing anti-*mqo* and anti-*xapR* sRNA.	This study	
pWAS-anti-mqo-anti-purB	pWAS derivative containing anti-*mqo* and anti-*purB* sRNA.	This study	
pWAS-anti-mqo-anti-fabH	pWAS derivative containing anti-*mqo* and anti-*fabH* sRNA.	This study	
pWAS-anti-xapR-anti-purB	pWAS derivative containing anti-*xapR* and anti-*purB* sRNA.	This study	
pWAS-anti-xapR-anti-fabH	pWAS derivative containing anti-*xapR* and anti-*fabH* sRNA.	This study	
pWAS-anti-purB-anti-fabH	pWAS derivative containing anti-*purB* and anti-*fabH* sRNA.	This study	
pWAS-anti-fadR-anti-xapR	pWAS derivative containing anti-*fadR* and anti-*xapR* sRNA.	This study	MH488950
pWAS-anti-xapR-anti-hycI	pWAS derivative containing anti-*xapR* and anti-*hycI* sRNA.	This study	
pWAS-anti-fadR-anti-hycI	pWAS derivative containing anti-*fadR* and anti-*hycI* sRNA.	This study	

[§] Abbreviations: Ap, ampicillin; Km, kanamycin; Spc, spectinomycin; R, resistance; MCS, multiple cloning site.

[¶] Denote GenBank accession numbers for the plasmid sequences.

Table S5. The list of oligonucleotides used in this study.

Primer Name	**Sequence 5'-3'** [#]
Sgr_rppA_F	CTTTAAGAAGGAGATATACATATGGCGACCCTGTGCCGACC
Sgr_rppA_R	CTTGTCGACGGAGCTCGAATTCATTAGCCGGACAGCGCAACGC
Sco_rppA_F	CTTTAAGAAGGAGATATACATATGGCGACTTTGTGCAGACC
Sco_rppA_R	CTTGTCGACGGAGCTCGAATTCATTATGCCTGCCTCACCCTCC
Sma_rppA_F	CTTTAAGAAGGAGATATACATATGGCGACGCTGTGCAAACC
Sma_rppA_R	CTTGTCGACGGAGCTCGAATTCATTACGCCTCGTCGGTGCGGTG
Sen_rppA_F	CTTTAAGAAGGAGATATACATATGGCAGTTCTATGCACCCC
Sen_rppA_R	CTTGTCGACGGAGCTCGAATTCATTATCGGTTGCCTCCCGGG
Sp_rppA_F	CTTTAAGAAGGAGATATACATATGCGTGTCCCTGTGGCCGTC
Sp_rppA_R	CTTGTCGACGGAGCTCGAATTCATTACCAGCGCAGGAGGACGAATTC
Sac_rppA_F	CTTTAAGAAGGAGATATACATATGCCAAGGCTGTGCAAGCC
Sac_rppA_R	CTTGTCGACGGAGCTCGAATTCATTAGTTCGACGTGCCCGTGC
whiE_orfII_F	TTATTAGAATTCAATAATTTTGTTTAACTTTAAGAAGGAGATATAATGACAGACCAGCAGGTACG
whiE_orfII_R	TAATAAGCTTATTATGACACCACCTCGGCC
pTac_CDF_F	CGACTCCTGCATTAGGAAATGACTGCACGGTGCACCAATG
pTac_CDF_R	GCGTTTCACTTCTGAGTTCG
pCDF_pTac_IV_F	CGAACTCAGAAGTGAAACGCCTGAAACCTCAGGCATTTGAG
pCDF_pTac_IV_R	ATTTCCTAATGCAGGAGTCG
pTac_rppA_F	CAATTTCACACAGGAAACAGAATGGCGACCCTGTGCCGACC
pTac_rppA_R	CTCTAGAGGATCCCCGGGTACCATTAGCCGGACAGCGCAACGC
pTac_rppA_IV_F	GGTACCCGGGGATCCTCTAGAG
pTac_rppA_IV_R	TCTGTTTCCTGTGTGAAATTG
pTac_rppA_5'UTR_IV_R	GATGCTCCTTTCTTGTTATTGAAATTGTTATCCGCTCACAATTC
AaPCS_F	CTTTAAGAAGGAGATATACATATGAGTTCACTCTCCAACTCTC
AaPCS_R	CTTGTCGACGGAGCTCGAATTCATTACATGAGAGGCAGGCTGTG
AaOKS_F	CTTTAAGAAGGAGATATACATATGAGTTCACTCTCCAACGCTTC
AaOKS_R	CTTGTCGACGGAGCTCGAATTCATTACATGAGAGGCAGGCTGTG
AaPKS3_F	CTTTAAGAAGGAGATATACATATGGGTTCACTCTCCGACTCTAC
AaPKS3_R	CTTGTCGACGGAGCTCGAATTCATTACACAGGAGGCAGGCTATG
AaPKS3_mut_F	GCTCACCATCATTGGGCTCCGTGGCCCCAATG
AaPKS3_mut_R	CATTGGGGCCACGGAGCCCAATGATGGTGAGC
AaPKS4_F	CTTTAAGAAGGAGATATACATATGGGTTCACTCTCCAACTAC
AaPKS4_R	CTTGTCGACGGAGCTCGAATTCATTACACAGGGGGCAGGCTG
AaPKS5_F	CTTTAAGAAGGAGATATACATATGGGTTCGATCGCCGAG
AaPKS5_R	CTTGTCGACGGAGCTCGAATTCATTAGACAGGAGGCAGGCTG
pTac_His_rppA_F	CAATTTCACACAGGAAACAGAATGCACCATCACCATCACCATGCGACCCTGTGCCGACC

Primer Name	Sequence 5'-3' [#]
pTac_pBBR1_F	GACTGCACGGTGCACCAATG
pTac_pBBR1_R	GCGTTTCACTTCTGAGTTCG
pTac_pBBR1_IV_F	CGAACTCAGAAGTGAAACGCTGCCTAATGAGTGAGCTAAC
pTac_pBBR1_IV_R	CATTGGTGCACCGTGCAGTCAAAATTCGCGTTAAATTTTTG
pCES_rppA_F	GGTTGGTAGGAGTAGCATGGGATCCATGGCGACCCTGTGCCGACC
pCES_rppA_R	CCGAGGCCTAATTATAATGGATTAGCCGGACAGCGCAACGC
pCES_His_rppA_F	GGTTGGTAGGAGTAGCATGGGATCCATGCACCATCACCATCACCATGC
pCES_H36_IV_F	CCATTATAATTAGGCCTCGG
pCES_H36_IV_R	CCATGCTACTCCTACCAACC
zwf_F	CACACAGGAAACAGACCATGGCGGTAACGCAAACAGC
zwf_R	CAGGTCGACTCTAGAGGATCCATTACTCAAACTCATTCCAGGAAC
mdh_F	CACACAGGAAACAGACCATGAAAGTCGCAGTCCTCGG
mdh_R	CAGGTCGACTCTAGAGGATCCATTACTTATTAACGAACTCTTCGCC
fumA_F	CACACAGGAAACAGACCATGTCAAACAAACCCTTTCATTATC
fumA_R	CAGGTCGACTCTAGAGGATCCATTATTTCACACAGCGGGTGC
fumB_F	CACACAGGAAACAGACCATGTCAAACAAACCCTTTATCTAC
fumB_R	CAGGTCGACTCTAGAGGATCCATTACTTAGTGCAGTTCGCGC
fumC_F	CACACAGGAAACAGACCATGAATACAGTACGCAGCGAAAAAG
fumC_R	CAGGTCGACTCTAGAGGATCCATTAACGCCCGGCTTTCATAC
serA_F	CACACAGGAAACAGACCATGGCAAAGGTATCGCTGGAG
serA_R	CAGGTCGACTCTAGAGGATCCATTAGTACAGCAGACGGGCGC
serB_F	CACACAGGAAACAGACCATGCCTAACATTACCTGGTGC
serB_R	CAGGTCGACTCTAGAGGATCCATTACTTCTGATTCAGGCTGCC
serC_F	CACACAGGAAACAGACCATGGCTCAAATCTTCAATTTTAGTTC
serC_R	CAGGTCGACTCTAGAGGATCCATTAACCGTGACGGCGTTCG
tpiA_F	CACACAGGAAACAGACCATGCGACATCCTTTAGTGATG
tpiA_R	CAGGTCGACTCTAGAGGATCCATTAAGCCTGTTTAGCCGCTTC
pTrc_IV_F	GGATCCTCTAGAGTCGACCTG
pTrc_IV_R	CATGGTCTGTTTCCTGTGTG
pTac_6MSAS_IV_F	GCTGAGAAGCTTGCCAAATAATGGATCCTCTAGAGTCGACCTG
pTac_6MSAS_IV_R	CTGGGGATGTTTTCCCAGAGGGGTATGTAGAAGTTGCAGCGGAATGCATGAATTCTGTTTCCTGTGTGAAATTG
6MSAS_F_1	ACAGTGAATATGAATTCTCCAACG
6MSAS_F_2	CTCTGGGAAAACATCCCCAGCACCAGTCGGAACCCCTGGGACTGAGT ACAGTGAATATGAATTCTCCAACG
6MSAS_R	ATTATTTGGCAAGCTTCTCAGC
sfp_F	TAATAAGAATTCATGAAGATTTACGGAATTTATATG
sfp_R	TTATTAGAATTCTTATAAAAGCTCTTCGTACGAG
pTac_sfp_F	CTAGAGTCGACCTGCAGGCATGCCACTCCCGTTCTGGATAATG
pTac_sfp_R	CAAAACAGCCAAGCTTGCATGC

Primer Name	**Sequence 5'-3'** [#]
pBBR1TaC_F	GTTGACAATTAATCATCGGCTC
pBBR1TaC_R	ACTAGTAAAAGGCCATCCGTCAGGATG
pBBR1TaC_IV_F	GACGGATGGCCTTTTACTAGTGCCTGGGGTGCCTAATGAG
pBBR1TaC_IV_R	CGATGATTAATTGTCAACTGCTACGCCTGAATAAGTGATAATAAG
pTac_frag_F	GTTGACAATTAATCATCGGC
pTac_frag_R	CGTTTCACTTCTGAGTTCGG
pTaC_IV_F	CCGAACTCAGAAGTGAAACG
pTaC_IV_R	GCCGATGATTAATTGTCAAC
Cgl_accBC_F	CAATTTCACACAGGAAACAGAATTCGTGTCAGTCGAGACTAGGAAG
Cgl_accBC_R	CTCTAGAGGATCCCCGGGTACCATTACTTGATCTCGAGGAGAAC
Cgl_accD1_F	CAATTTCACACAGGAAACAGAATTCATGACCATTTCCTCACCTTTG
Cgl_accD1_R	CTCTAGAGGATCCCCGGGTACCATTACAGTGGCATGTTGCCGTG
pTac_HindIII_frag_F	GAGTCGACCTGCAGGCATGCATTGACAATTAATCATCGGCTCG
pTac_HindIII_frag_R	CTCATCCGCCAAAACAGCCAAGCTT
aceEF_F	CAATTTCACACAGGAAACAGAATTCATGTCAGAACGTTTCCCAAATG
aceEF_R	CTCTAGAGGATCCCCGGGTACCATTACATCACCAGACGGCGAATG
lpd_F	CAATTTCACACAGGAAACAGAATTCATGAGTACTGAAATCAAAACTC
lpd_R	CTCTAGAGGATCCCCGGGTACCATTACTTCTTCTTCGCTTTCGG
pTac_SalI_frag_F	GTACCCGGGGATCCTCTAGAGTTGACAATTAATCATCGGCTCG
pTac_SalI_frag_R	CAAGCTTGCATGCCTGCAGGTCGAC
gapA_F	CAATTTCACACAGGAAACAGAATTCATGACTATCAAAGTAGGTATCAAC
gapA_R	CTCTAGAGGATCCCCGGGTACCATTATTTGGAGATGTGAGCGATC
pgk_F	CAATTTCACACAGGAAACAGAATTCATGTCTGTAATTAAGATGACCGATC
pgk_R	CTCTAGAGGATCCCCGGGTACCATTACTTCTTAGCGCGCTCTTCG
acs_F	CAATTTCACACAGGAAACAGAATTCATGAGCCAAATTCACAAACAC
acs_R	CTCTAGAGGATCCCCGGGTACCATTACGATGGCATCGCGATAG
SeTAL_F	GAATTGTGAGCGGATAACAAAGACCGAGGAAAAGGAGCATCGCAAATGACGCAGGTCGTGGAACGTC
SeTAL_R	TAGAGGATCCCCGGGTACTCATCCGAAATCCTTCCCGTC
pTrc99A_IV_F	GTACCCGGGGATCCTCTAG
pTrc99A_IV_R	TTGTTATCCGCTCACAATTC
HisTAL_F	GAGGAAAAGGAGCATCGCAAATGCACCATCATCATCATCATACGCAGGTCGTGGAACGTC
pTrcTAL_IV_R	TTGCGATGCTCCTTTTCCTC
TrxTAL_F	CCTCGACGCTAACCTGGCGACGCAGGTCGTGGAACGTC
SeTAL_frag_R	TCATCCGAAATCCTTCCCGTC
TrxA_F	ATGAGCGATAAAATTATTCACCTG
TrxA_R	CGCCAGGTTAGCGTCGAGG

Primer Name	**Sequence 5'-3'** [#]
TrxA_ext_F	AGACCGAGGAAAAGGAGCATCGCAAATGAGCGATAAAATTATTCACCTG
pTac_frag_NheI_F	GTAAGCCAGTATACACTCCGGACTGCACGGTGCACCAATG
pTac_frag_NheI_R	CTGTTGGGCGCCATCTCCTTGTGTAGAAACGCAAAAAGGCCATC
At4CL1_F	CAATTTCACACAGGAAACAGACATATGGCGCCACAAGAACAAGC
At4CL1_R	CTCTAGAGGATCCCCGGGTACCATTACAATCCATTTGCTAGTTTTG
At4CL1_mut_F_1	CACAGCGATGACGTCCTACTCTGTGTTTTG
At4CL1_mut_R_1	CAAAACACAGAGTAGGACGTCATCGCTGTG
At4CL1_mut_F_2	CTCTTTCGAGGAAACAACCCGGTGAG
At4CL1_mut_R_2	CTCACCGGGTTGTTTCCTCGAAAGAG
At4CL1_mut_F_3	GATTGAAAGAACTTGTCAAGTATAAAGG
At4CL1_mut_R_3	CCTTTATACTTGACAAGTTCTTTCAATC
At4CL3_F	CAATTTCACACAGGAAACAGACATATGATCACTGCAGCTCTACAC
At4CL3_R	CTCTAGAGGATCCCCGGGTACCATTAACAAAGCTTAGCTTTGAGG
At4CL4_F	CAATTTCACACAGGAAACAGACATATGGTGCTCCAACAACAAACG
At4CL4_R	CTCTAGAGGATCCCCGGGTACCATTATTTAGAGCACATGGTTTCC
Sc4CL_F	CAATTTCACACAGGAAACAGACATATGTTCCGCAGCGAGTACGC
Sc4CL_R	CTCTAGAGGATCCCCGGGTACCATTATCGCGGCTCCCTGAGCTGTC
Sc4CL_mut_F	GTACATCGTCAGCGGCGCCGCCCCGCTCGACG
Sc4CL_mut_R	CGTCGAGCGGGGCGGCGCCGCTGACGATGTAC
VvSTS_F	CAATTTCACACAGGAAACAGACATATGGCAAGTGTCGAGGAATTC
VvSTS_R	CTCTAGAGGATCCCCGGGTACCATTAATTGGTAACCATCGGAATGG
pTac_PvuII_frag_F	GCACATCCCCCTTTCGCCAGGACTGCACGGTGCACCAATG
pTac_PvuII_frag_R	CCTCTTCGCTATTACGCCAGTGTAGAAACGCAAAAAGGCCATC
VvSTS_opr_F	GAGTCGACCTGCAGGCATGCAATTTCACACAGGAAACAGA
VvSTS_opr_R	CAAAACAGCCAAGCTTGCATG
At4CL1_fus_F	TTTCACACAGGAAACAGACATATG
At4CL1_fus_R	GAATTCCTCGACACTTGCCATACTACCACCACCCAATCCATTTGCTAGTTTTG
At4CL1m_PstI_F	GATCCTCTAGAGTCGACCTGCAGGACTGCACGGTGCACCAATG
At4CL1m_PstI_R	CAAAACAGCCAAGCTTGCATG
At4CL1_KpnI_F	AGACAGGGTACCATGGCGCCACAAGAACAAG
At4CL1_OE_R	ATGTATATCTCCTTCTTAAAGTTAATTACAATCCATTTGCTAGTTTTGCCC
AtCHI_OE_F	TTAACTTTAAGAAGGAGATATACATATGTCTTCATCCAACGCCTGC
AtCHI_BamHI_R	AGACAGGGATCCTCAGTTCTCTTTGGCTAGTTTTTCC
PhCHS_BamHI_F	AGAGAGGATCCATAACAATTCCCCATCTTAG
PhCHS_XbaI_R	AGAGATCTAGATTAGGTAGCCACACTATGCAGAACC
pTrc_NcoI_IV_R	GAAACTGCTTGTTCTTGTGGCGCCATGGTCTGTTTCCTGTGTG
pTrc_PstI_IV_F	CTAATCTAGAGTCGACCTGCAGGCATGCAAGCTTG
sRNAdouble_IV_F	GCACATGTTTGATTTATAAGGG

Primer Name	**Sequence 5'-3'** [#]
sRNAdouble_IV_R	CAGCACATTTGAGATCTAGTGG
sRNAdouble_F	CACTAGATCTCAAATGTGCTGGAATTCTAACACCGTGCGTG
sRNAdouble_R	CCTTATAAATCAAACATGTGCGGCGAATTGGGTACCTATAAAC
sRNAdouble_IV_F_1	GCTTACAATTTAGGTGGCAC
sRNAdouble_IV_R_1	GTTAATATTTTGTTAAAATTCGCG
sRNAdouble_F_1	GAATTTTAACAAAATATTAACGAATTCTAACACCGTGCGTG
sRNAdouble_R_1	GTGCCACCTAAATTGTAAGCGGCGAATTGGGTACCTATAAAC

[#] Underlines denote restriction sites.

References

1. Sambrook J, Russell DW (2001) *Molecular Cloning: A Laboratory Manual* (Cold Spring Harbor Lab Press, NY).
2. Gibson DG, *et al.* (2009) Enzymatic assembly of DNA molecules up to several hundred kilobases. *Nature Methods* 6:343-345.
3. Lee SY, *et al.* (2008) Recombinant microorganism having an ability of using sucrose as a carbon source. US patent 20110269183.
4. Seo SW, *et al.* (2013) Predictive design of mRNA translation initiation region to control prokaryotic translation efficiency. *Metab Eng* 15:67-74.
5. Esposito D, Chatterjee DK (2006) Enhancement of soluble protein expression through the use of fusion tags. *Curr Opin Biotechnol* 17:353-358.
6. Na D, *et al.* (2013) Metabolic engineering of *Escherichia coli* using synthetic small regulatory RNAs. *Nat Biotechnol* 31:170-174.
7. Yoo SM, Na D, Lee SY (2013) Design and use of synthetic regulatory small RNAs to control gene expression in *Escherichia coli*. *Nat Protoc* 8:1694-1707.
8. Lee Y, Lee SY (1996) Enhanced production of poly(3-hydroxybutyrate) by filamentation-suppressed recombinant *Escherichia coli* in a defined medium. *J Environ Polym Degrad* 4:131-134.
9. Ko KC, Han Y, Cheong DE, Choi JH, Song JJ (2013) Strategy for screening metagenomic resources for exocellulase activity using a robotic, high-throughput screening system. *J Microbiol Methods* 94:311-316.
10. Armando JW, Boghigian BA, Pfeifer BA (2011) LC-MS⁄MS quantification of short-chain acyl-CoA's in *Escherichia coli* demonstrates versatile propionyl-CoA synthetase substrate specificity. *Lett Appl Microbiol* 54:140-148.
11. Bennett BD, *et al.* (2009) Absolute metabolite concentrations and implied enzyme active site occupancy in Escherichia coli. *Nat Chem Biol* 5:593-599.
12. Pfeifer BA, Admiraal SJ, Gramajo H, Cane DE, Khosla C (2001) Biosynthesis of complex polyketides in a metabolically engineered strain of *E. coli*. *Science* 291:1790-1792.
13. Datsenko KA, Wanner BL (2000) One-step inactivation of chromosomal genes in *Escherichia coli* K-12 using PCR products. *Proc Natl Acad Sci U S A* 97:6640-6645.
14. Song CW, Lee SY (2013) Rapid one-step inactivation of single or multiple genes in *Escherichia coli*. *Biotechnology Journal* 8:776-784.
15. Orth JD, *et al.* (2011) A comprehensive genome-scale reconstruction of *Escherichia coli* metabolism—2011. *Mol Syst Biol* 7:535.
16. Park JM, *et al.* (2012) Flux variability scanning based on enforced objective flux for identifying gene amplification targets. *BMC Syst Biol* 6:106.
17. Ebrahim A, Lerman JA, Palsson BØ, Hyduke DR (2013) COBRApy: COnstraints-Based Reconstruction and Analysis for Python. *BMC Syst Biol* 7.
18. Austin MB, *et al.* (2004) Crystal structure of a bacterial type III polyketide synthase and enzymatic control of reactive polyketide intermediates. *J Biol Chem* 279:45162-45174.
19. Funa N, Funabashi M, Yoshimura E, Horinouchi S (2005) A novel quinone-forming monooxygenase family involved in modification of aromatic polyketides. *J Biol Chem* 280:14514-14523.
20. Liao H, *et al*. (2012) Microorganisms and methods for the production of fatty acids and fatty acid derived products. US patent 20140051136.

21. Lynch MD, *et al*. (2011) Microbial production of chemical products and related compositions, methods and systems. US patent 20140330032.
22. Krauser S, Kiefer P, Heizle E (2012) Multienzyme whole-cell in situ biocatalysis for the production of flaviolin in permeabilized cells of *Escherichia coli*. *ChemCatChem* 4:786-788.
23. Gerdes SY, *et al.* (2003) Experimental determination and system level analysis of essential genes in *Escherichia coli* MG1655. *J Bacteriol* 185:5673-5684.
24. Haverkorn van Rijsewijk BR, Nanchen A, Nallet S, Kleijn RJ, Sauer U (2011) Large-scale ^{13}C-flux analysis reveals distinct transcriptional control of respiratory and fermentative metabolism in *Escherichia coli*. *Mol Syst Biol* 7:477.
25. Zha W, Rubin-Pitel SB, Shao Z, Zhao H (2009) Improving cellular malonyl-CoA level in *Escherichia coli* via metabolic engineering. *Metab Eng* 11:192-198.
26. Raman S, Rogers JK, Taylor ND, Church GM (2014) Evolution-guided optimization of biosynthetic pathways. *Proc Natl Acad Sci U S A* 111:17803-17808.
27. Xiong D, *et al.* (2017) Improving key enzyme activity in phenylpropanoid pathway with a designed biosensor. *Metab Eng* 40:115-123.
28. Li Y, Kim JI, Pysh L, Chapple C (2015) Four isoforms of *Arabidopsis* 4-coumarate:CoA ligase have overlapping yet distinct roles in phenylpropanoid metabolism. *Plant Physiol* 169:2409-2421.
29. Kaneko M, Ohnishi Y, Horinouchi S (2003) Cinnamate:coenzyme A ligase from the filamentous bacterium *Streptomyces coelicolor* A3(2). *J Bacteriol* 185:20-27.
30. Li M, *et al.* (2015) De novo production of resveratrol from glucose or ethanol by engineered *Saccharomyces cerevisiae*. *Metab Eng* 32:1-11.
31. Kim B, Binkley R, Kim HU, Lee SY (2018) Metabolic engineering of *Escherichia coli* for the enhanced production of L-tyrosine. *Biotechnol Bioeng* In press. doi: 10.1002/bit.26797.
32. Watts KT, Lee PC, Schmidt-Dannert C (2006) Biosynthesis of plant-specific stilbene polyketides in metabolically engineered *Escherichia coli*. *BMC Biotechnol* 6:22.
33. Vogel G, Lynen F (1975) 6-Methylsalicylic acid synthetase. *Methods Enzymol* 43:520-530.
34. Beltrán-García MJ, *et al.* (2014) Singlet molecular oxygen generation by light-activated DHN-melanin of the fungal pathogen *Mycosphaerella fijiensis* in black Sigatoka disease of bananas. *PLoS One* 9:e91616.
35. Mizuuchi Y, *et al.* (2009) Novel type III polyketide synthases from *Aloe arborescens*. *FEMS J* 276:2391-2401.
36. Kroese DP, Taimre T, Botev ZI (2011) *Handbook of Monte Carlo Methods* (John Wiley & Sons, NY).
37. Hanahan D (1983) Studies on transformation of *Escherichia coli* with plasmids. *J Mol Biol* 166:557-580.
38. Fernández-González C, *et al.* (1996) Construction of L-lysine-overproducing strains of *Brevibacterium lactofermentum* by targeted disruption of the *hom* and *thrB* genes. *Appl Microbiol Biotechnol* 46:554-558.
39. Elliott SJ, Nandapalan N, Chang BJ (1991) Production of type 1 fimbriae by *Escherichia coli* HB101. *Microb Pathog* 10:481-486.
40. Blattner FR, *et al.* (1997) The complete genome sequence of *Escherichia coli* K-12. *Science* 277:1453-1462.
41. Bolivar F, *et al.* (1977) Construction and characterization of new cloning vehicles. II. A multipurpose cloning system. *Gene* 2:95-113.

42. Hayashi K, *et al.* (2006) Highly accurate genome sequences of *Escherichia coli* K-12 strains MG1655 and W3110. *Mol Syst Biol* 2:2006.0007.
43. Archer CT, *et al.* (2011) The genome sequence of *E. coli* W (ATCC 9637): comparative genome analysis and an improved genome-scale reconstruction of *E. coli*. *BMC Genomics* 12:9.
44. Caspi R, *et al.* (2014) The MetaCyc database of metabolic pathways and enzymes and the BioCyc collection of Pathway/Genome Databases. *Nucleic Acids Res* 42:D459-D471.
45. Kovach ME, *et al.* (1995) Four new derivatives of the broad-host-range cloning vector pBBR1MCS, carrying different antibiotic-resistance cassettes. *Gene* 166:175-176.
46. Yim SS, An SJ, Kang M, Lee J, Jeong KJ (2013) Isolation of fully synthetic promoters for high-level gene expression in *Corynebacterium glutamicum*. *Biotechnol Bioeng* 110:2959-2969.
47. Kovach ME, Phillips RW, Elzer PH, Roop II RM, Peterson KM (1994) pBBR1MCS: a broad-host-range cloning vector. *BioTechniques* 16:800-802.